Università degli Studi di Cagliari

DOTTORATO DI RICERCA

Medicina Molecolare e Traslazionale

Ciclo XXXI

TITOLO TESI

Neuroanatomy of energy and glucose regulation: the novel TLQP-21 and TLQP-62 peptides

Settore/i scientifico disciplinari di afferenza

BIO/16 ANATOMIA UMANA

Presentata da: Dott. Carlo Lisci

Coordinatore Dottorato: Prof. Amedeo Columbano

Tutor: Prof. G-Luca Ferri

Esame finale anno accademico 2017 – 2018
Tesi discussa nella sessione d'esame Febbraio 2019

1. INTRODUCTION

1.1 VGF

vgf is the (non-acronymic) name given by Andrea Levi (1985) to a gene that was originally recognized as one of the most strongly induced genes when PC12 cells switched to a neuronal phenotype upon treatment with Nerve Growth Factor (NGF), the first one identified of neuronal growth factors, discovered by Rita Levi-Montalcini (1968). NGF belongs to the class of neurotrophins, which includes other growth factors such Brain Derived Neurotrophic Factor (BDNF); Neurotrophin 3 (NT3); and Neurotrophin 4/5 (NT4/5).

The above neurotrophins are proteins that promote the proliferation, differentiation, survival and maintenance of the differentiation of central neurons, as well as inducing functional modulations of their phenotype.

The neurotrophins have also significant neuroprotective effects that they exert on various neuronal types, making them interesting for a possible therapeutic use in neurodegenerative diseases.

One of the most used cell lines to study neurotrophins and differentiation neuronal is a cell line derived from rat pheochromocytoma, called PC12. Its cells are round and small (5-10μm) in the absence of NGF, show a small amount of cytoplasm and duplicate in just over 48 hours. PC12 cells derive from adrenal medullary cells, do not require NGF to survive, and on their own show an epithelioid appearance, with growth at confluence. The addition of NGF to the culture medium induces the differentiation of PC12 cells to a neuronal phenotype, characterized by the extension of neurites. Such modification is associated with, and is largely mediated by the expression of specific genes.

The genes induced by NGF have been divided into two categories based on the timing necessary for their induction:

- "Immediate-Early" genes: induced at a very early stage, and largely coding for transcription factors. Such genes are considered to be part of the non-specific cellular response system (Herschman, 1989);

- "Delayed-Early" genes: induced with delayed kinetics, after the accumulation of "Immediate-Early" gene products.

The *vgf* gene belongs to the latter category and its expression depends on it essential from protein synthesis. An increase in *vgf* mRNA level is evident in PC12 cells about 30 to 60 minutes after administration of NGF in PC12, with a high plateau (50 times baseline values) after 5 to 8 hours (Levi et al., 1985).

In addition basic Fibroblast Growth Factor (bFGF) (Miyatake et al., 1993), interleukin 6 (IL-6), cAMP, BDNF, EGF (Epidermal Growth Factor), insulin and cellular depolarization (Salton et al., 1991; Possenti et al., 1992; Hawley et al., 1992) have proven effective in inducing *vgf* in PC12 cells and/or in the nervous system. The latter factors, however, induce the *vgf* gene at lower levels (5-10 times baseline values) compared to NGF. Further studies have shown that by administering NGF to cells for longer times (9-25 hours) the vgf mRNA decreases and become less stable (Baybis and Salton, 1992).

1.2 Structure of the *vgf* gene

The *vgf* gene was originally identified in PC12 cells treated with NGF. The gene is present as a single copy (Salton et al., 1991) and is mapped in man on chromosome 7q22 (Canu et al., 1997), while in mouse it is found on chromosome 5 (Hahm et al., 1999). The coding region of the gene consists of an exon, and an intron that is found in position 5' (Salton et al., 1991; Hawley et al., 1992; Possenti et al., 1992).

Although there is a certain trascriptional heterogeneity, with the production of two different mRNAs, the coding portion of the gene is not involved , and both mRNAs encode for the precursor protein called VGF.

Deletion of the mouse *vgf* gene (knockout) resulted in thin, small, hyperactive and hypermetabolic animals (Hahm et al. 1999), with an apparent derangement of hypothalamic outflow pathways

regulating peripheral metabolic tissues and energy homoeostasis (Hahm et al. 2002). More recently, in a second strain of knock out mice, an increased sympathetic appeared to induce increased lipolysis, decreased lipogenesis and brown adipocyte differentiation in white adipose tissue (WAT) (Watson et al. 2009). In addition, VGF Knock-out mice showed an increase in insulin sensitivity, in association with reduced glycogen stores in the liver (Watson et al.; 2005).

1.3 The primary sequence of *vgf*

The primary translation product derived from the *vgf* gene is a protein called VGF, or sometime, in the past, pro-VGF to underline its predicted and subsequently demonstrated role as precursor of polypeptide products. It is composed of 617 amino acids residues (aa) in rat and mouse (Salton et al., 1991), 615 aa in the human species (see Fig. 1 for the primary sequence of VGF).

Between the human and rat / mouse sequences there is an about 85% homology (see: Ferri et al., 2011, for a review). Further studies have shown that human *vgf* is also closely conserved compared to the one found for other species, including bovine (*Bos taurus*). In the bovine neurohypophysis a peptide corresponding to the C-terminal sequence of VGF has been found and called peptide V or AQEE-30, with the same aa in human (Liu et al., 1994). Further studies have also found sequence similarities in primates and equines (*Review*: Ferri et al., 2011).

The primary amino acid sequence has some noteworthy peculiarities:

- A leading sequence (signal peptide) composed of 22 aa, with a hydrophobic region in the amino terminal region, which promotes translocation to the endoplasmic reticulum;
- Numerous stretches containing two or more basic residues (Arg and / or Lys, or R / K in single letter notation), or related sequences (Arg-Pro-Arg, or R-P-R, at position 555). These sites have been demonstrated as proteolytic cleavage sites;
- An Ala-Gly-Arg-Arg sequence (A-G-R-R) showing a glycine residue immediately upstream of a

potential cleavage site. This sequence suggests that it is possible that a peptide is produced this region, with an amide group at its C-terminal end. In fact, C-terminal amidation is a functional hallmark of many bioactive peptides, e.g. Gastrin, NPY, PYY;

- A high proline content (11%). This feature makes VGF similar to the neuroendocrine proteins called chromogranins;
- A high content of aspartic acid (14%) and glutamic acid in a restricted area of the molecule that make it acidic.

The primary sequence of VGF shows no distinct similarity with other known gene products. Hence, VGF may represent the precursor of a novel family of peptides. VGF, as mentioned above, is often associated with the chromogranins family, in relation to their common selective localization in neuro-endocrine secretory granules. The VGF protein, and / or its cleavage products (VGF peptides), may be secreted following the regulated path. Such process involves the splitting into peptide fragments through proteolytic processes. Such cleavage is favored by enzymes that recognize specific sequences upstream or downstream, possibly even at some distance from the dibasic site (Salton et al., 1991), during their transport in secretory vesicles, with where they are accumulated in the same cells and / or secreted in relation to stimuli (Possenti et al., 1999).

Fig. 1) Comparison of the human and mouse VGF polypeptide sequences. " * " indicates the position which have a single, fully conserved residue. " : " indicates conservation between groups of strongly similar properties scoring > 0.5 in the Gonnect PAM 250 matrix. " . " indicates conservation between groups of weakly similar properties scoring < 0.5 in the Gonnet PAM 250 matrix. Clusters of basic amino acids, which represent potential cleavage sites, are boxed. Sequence identity was > 85%

```
Human MKALRLSASALFC-LLLINGLGAAPPGRPEAQPPPLSSEHKEPVAGDAVPGPKDGSAPEV 59
Mouse MKTFTLPASVLFCFLLLIQGLGAAPPGRPDVFPPPLSSEHNGQVAEDAVSRPKDDGVPEV 60
      **:: *.**.*** ****:**********:. ********:  ** ***. ***...***

Human RGARNSEPQDEGELFQGVDPRALAAVLLQALDRPASPP-APSGSQQGPEEEAAEALLTET 118
Mouse RAARNPEPQDQGELFQGVDPRALASVLLQALDRPASPPSVPGGSQQGTPEEAAEALLTES 120
      *.***.****:*************:************* .*.*****. **********:

Human VRSQTHSLPAPESPEP-AAPPRPQTPENGPEASDPSEELEALASLLQELRDFSPSSAKRQ 177
Mouse VRSQTHSLPAPEIQAPAVAPPRPQTQDRDPEEDDRSEELEALASLLQELRDFSPSNAKRQ 180
      ************   * .******* :..** .* ********************.****

Human QETAAAETETRTHTLTRVNLESPGPERVWRASWGEFQARVPERAPLPPPAPSQFQARMPD 237
Mouse QETAAAETETRTHTLTRVNLESPGPERVWRASWGEFQARVPERAPLPPPVPSQFQARMSE 240
      ************************************************.********.:

Human SGPLPETHKFGEGVSSPKTHLGEALAPLSKAYQGVAAPFPKARRPESALLGGSEAGERLL 297
Mouse SAPLPETHQFGEGVSSPKTHLGETLTPLSKAYQSLGGPFPKVRRLEGSFLGGSEAGERLL 300
      *.******:***************:*:*******.:..****.**  *.::***********

Human QQGLAQVEAGRRQAEATRQAAAQEERLADLASDLLLQYLLQGGARQRGLGGRGLQEAAEE 357
Mouse QQGLAQVEAGRRQAEATRQAAAQEERLADLASDLLLQYLLQGGARQRDLGGRELQETQQE 360
      **********************************************.**** ***: :*

Human RESAREEEEAEQERRGG-EERVGEEDEEAAEAEAEAEEAERARQNALLFAEEEDGEAGAE 416
Mouse RENEREEE-AEQERRGGGEDDVGEEDEEAAEAEAEAEEAERARQNALLFAEEEDGEAGAE 419
      **. **** ********** *: ************************************

Human DKRSQEETPGHRRKEAEGTEEGGEEEDD-EEMDPQTIDSLIELSTKLHLPADDVVSIIEE 475
Mouse DKRSQEEAPGHRRKDAEGAEEGGEEDDDDEEMDPQTIDSLIELSTKLHLPADDVVSIIEE 479
      *********:*******:***:******:** ********************************

Human VEEKRKRKKNAPPEPVPPPRAAPAPTHVRSPQPPPPAPAPARDELPDWNEVLPPWDREED 535
Mouse VEEKRKRKKNAPPEPVPPPRAAPAPTHVRSPQPPP--PAPARDELPDWNEVLPPWDREED 537
      ***********************************  ************************

Human EVYPPGPYHPFPNYIRPRTLQPPSALRRRHYHHALPPSRHYPGREAQARRAQEEAEAEER 595
Mouse EVFPPGPYHPFPNYIRPRTLQPPASSRRRHFHHALPPARHHPDLEAQARRAQEEADAEER 597
      **:************************:: ****:******:**:*. ********:***:***

Human RLQEQEELENYIEHVLLRRP 615
Mouse RLQEQEELENYIEHVLLHRP 617
      *****************:**
```

It has been shown that the levels of VGF mRNA increase in the arcuate nucleus in response to fasting, with differential modulations in NPY and POMC neurons (Hahm et al., 1999; Hahm et al., 2002). The same happens for VGF peptides (used an antibody for the C-terminal fragment of the VGF precursor) especially in NPY neurons (Saderi et al., 2014). Much of the information for a role of *vgf* in nutrition and energy homeostasis derive from reports on VGF-/- with a deranged *vgf* gene (knock-out) as obtained in 1999 by Salton et al. The research group of prof. Salton has developed and studied two different models of VGF Knock-in (KI) mice. In one of these the whole sequence of human VGF (hVGF) had been used, while in the other the C-terminal portion of the sequence had been eliminated (hSNP). It turned out that hVGF mice had more fat accumulation than those hSNP animals. These results would focus on a key role of the C-terminal portion in the regulation of energy metabolism and adiposity (Sadahiro et al., 2015).

VGF deficient mice were indistinguishable from wild type ones at birth, but showed a reduced growing curve resulting in smaller dimension than wild type littermates. By postnatal day 3 (PND3), VGF mutant pups weighed 10–20% less than controls (wild type); by PND21, 40–60% less than wild types. After weaning, VGF mutant mice maintained a body weights about 50–70% of wild type animals. In addition, VGF deficient mice were hypermetabolic showing approximately 50% more O_2 consumption than wild type ones. Importantly, absolute daily food intake (grams per animal) was similar to that of wild type mice, while it was higher in knock-out animals when normalized per body weight. On the contrary, comparable hyperphagic responses (daily food intake) were noted following a 24 h fast. These changes in metabolic and nutritional parameters are paralleled by a peculiar endocrine and hematological profile (Hahm et al., 1999). The same KO mice were resistant to obesity induced by a high fat diet, as well as to that induced by thioglucose , which in normal mice causes hyperphagia and obesity (Hahm et al., 2002). The research group of prof. Salton has developed and studied two different models of VGF Knockin (KI) mice. In one of these the whole sequence of human VGF (hVGF) had

been used, while in the other the C-terminal portion of the sequence had been eliminated (hSNP). It turned out that hVGF mice had more fat accumulation than those hSNP animals. These results would focus on a key role of the C-terminal portion in the regulation of energy metabolism and adiposity (Sadahiro et al., 2015).

1.4 Post-transduction processing of VGF

As already mentioned above, the VGF protein has numerous pairs of basic amino acids. These are considered sites of cleavage, which occurs thanks to specific convertases (PC1 and PC1/3).

The proteolytic processing of the VGF protein determines the formation of different VGF-peptides, that are been, over the years, identified and isolated (Fig. 2).

Fig. 2) VGF peptides bioactivity

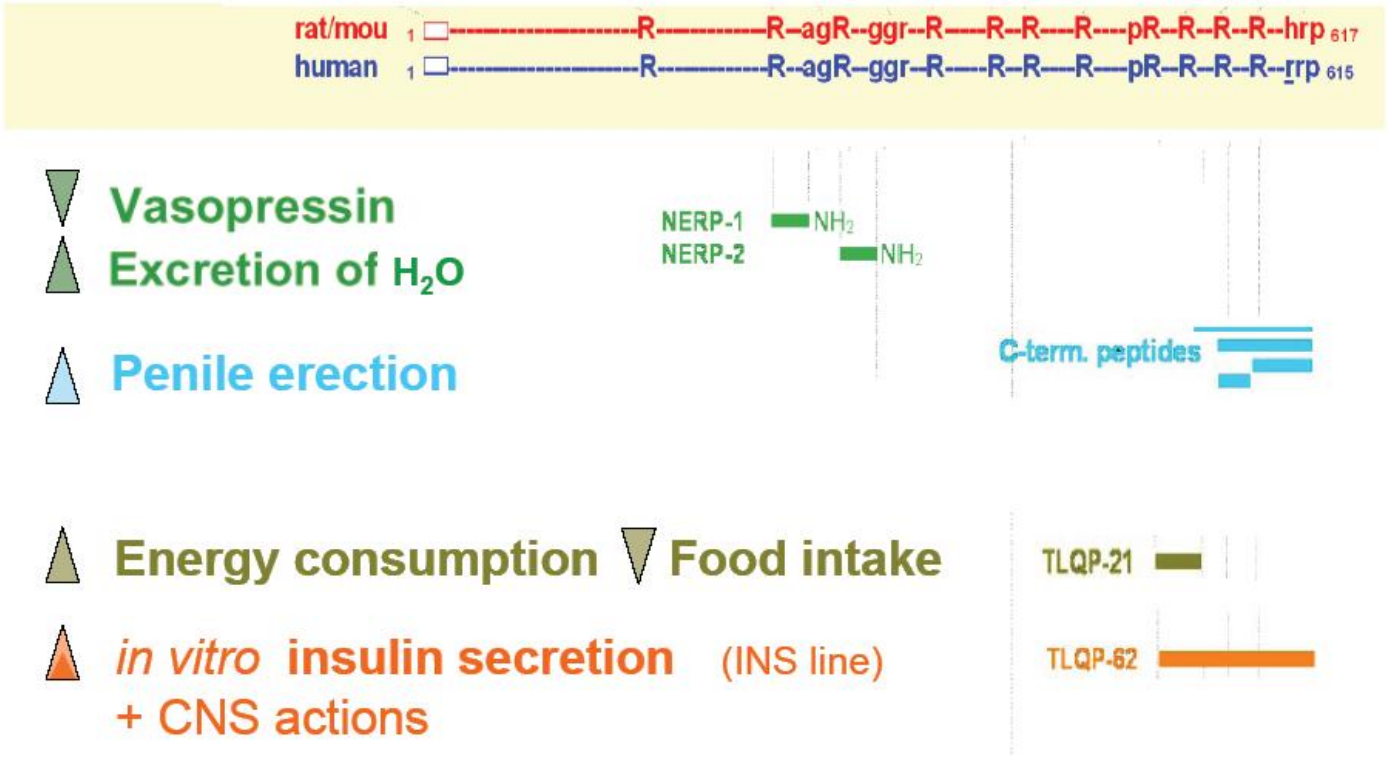

A key tool has been the production of highly specific antibodies, directed against narrow selected aminoacidic segments based on the primary sequence of VGF and on the potential cleavage, or cleavage-amidation sites mentioned above (*Review*: Ferri et al., 2011).

Among these, in particular an antibody directed against the C-terminal sequence of the protein (rat/mouse sequence), which revealed the presence not only of a high molecular weight polypeptide (90 kDa), corresponding to the whole protein, but also the presence of smaller peptides (about 20 kDa and 10 kDa, respectively) in brain homogenates, as well as in primary cultures of cerebellar granules, and in some endocrine tissues, including hypophyseal and hypothalamic cell lines, as well as pancreatic cell lines (Possenti et al., 1999; Trani et al., 1995).

The C-terminal region of VGF is characterized by considerable conservation of the sequence between species. In fact we observe a single amino acid substitution at the -3 position, between the human sequence in which there is an arginine residue (Arg_{613}), and that of rat or mouse, in which there is a histidine residue (His_{615}) (Salton et al., 2000). Using immunopurification procedures based on the aforementioned antibody in HPLC-mass and mass-mass, various low molecular weight peptides from rat brain extracts were identified, isolated and sequenced.

These peptides are produced through the cleavage of a unusual, specific site $R_{553}P_{554}R_{555}$ (numbering corresponding to the sequence of the rat), located in a domain relatively close to the C-terminus of VGF (Trani et al., 2002), and include a family of peptides called TLQP, because all contain this sequence. Since the TLQP peptides are the focus of this thesis, they will be described in details in a separated section.

In relation to the human gene sequence, it is interesting to remember how, already long time ago, the **AQEE-30** peptide, also called "peptide V", has been identified from extracts of bovine pituitary posterior (Liu et al., 1994). This peptide includes the 30 amino acid residues up to the C-terminal end of VGF. The identification of this peptide not only confirms how the bovine sequence of VGF is in this

region virtually identical to the human one, but also establishes that this peptide is a natural *in vivo* cleavage product of VGF, which is actually biosynthesised and likely released in the animal. More recent works in the field of proteomics have identified two bioactive peptides called **NERP-1** and **NERP-2**. This discovery occurred by analyzing TT cells of human thyroid carcinoma. The name is an acronym that stands for Neuroendocrine Regulatory Peptides 1 and 2. They are amidated peptides and derive from a distinct VGF protein region (Yamaguchi et al., 2007).

Two other recently identified peptides are: the one with **ERVW** sequence in its own extreme C-terminal and QQET sequence at its N-terminal end, this fragment it is called NERP-3, or **QQET-30**; the other one is a peptide with PTHV sequence at its C-terminal end and NAPP sequence at its N terminal end, called NERP-4, or **NAPP-19**. Both of these latter peptides, QQET-30 and NAPP-19, have been found by our own laboratory using HPLC-ESI-MS approaches in fractions from human plasma (D'Amato et al., 2015). NAPP-19 was also found in prefrontal cortex extracts from mice $Cpe^{fat/fat}$ (Lim et al., 2006; Zhang et al., 2008). The QQET-30 peptide was identified in rat intestine and brain acid extracts (Fujihara et al., 2012). This fragment was more abundant in the brain and in the posterior pituitary than in the intestine.

Fragments close to the N-terminus of VGF have been recognized in the liquid human cerebrospinal (Stark et al., 2001). Some of them are reduced in patients suffering from Alzheimer's disease (Carrette et al., 2003) and other neurodegenerative diseases, or altered with possible increase in carriers of schizophrenia or its prodromes (Huang et al., 2006, 2007).

1.5 Biological actions and activities of VGF peptides

The peptides above described have different biological activities. The peptides deriving from the C terminal portion of proVGF were the first studied *in vivo*.

Injecting into paraventricular hypothalamic nuclei of peptides from regions near the C-terminus of VGF ($VGF_{577-617}$ or shorter peptides within said sequence) resulted in erection in rats, by excitation mediated by nitric oxide through an oxytocinergic pathway (Succu et al., 2004; Succu et al., 2005). A possible role in the regulation of synaptic plasticity was found after treatment of PC12 cells with the C-terminal AQEE-30 peptide, or with infusion of the latter in the dentate gyrus of the rat hippocampus. In both cases, the peptide induced the expression of specific genes involved in synaptogenesis, in synaptic remodeling or in the stimulation of growth factors (Hunsberger et al., 2007).

NERP-1 and NERP-2 injected i.c.v., resulted in suppressing the release of vasopressin in plasma, whereas i.c.v. antibodies against the aforementioned peptides inhibited the reduction of vasopressin levels in response to water re-intake after dehydration. These responses suggest a possible role of these peptides in the physiological control of vasopressin-mediated water homeostasis (Yamaguchi et al., 2007). According to this hypothesis, an increase in NERP-1 and 2 in the median eminence and a decrease in plasma level in conditions of increased plasma osmolarity has been demonstrated (D'Amato et al., 2012). NERP-2 could also act on insulin secretion (Moin et al., 2012). The latter peptide would have further implications in the regulation of metabolism, in fact injected *i.c.v.* in rats, it induces an increase in food intake, locomotor activity and body temperature (Toshinai et al., 2010).

The NERP-3 peptide, on the other hand, on posterior pituitary preparations would induce a significant release of vasopressin (ADH), so it could be an autocrine activator in the posterior pituitary of ADH release, involved in regulating body hydrosaline in one direction "alternative" to that operated by NERP-1 and 2 (Fujihara et al., 2012)

1.5.1 TLQP peptides: localization and biological activities

Using an antibody able to recognise the TLQP sequence, generally different antisera are used against specific peptides and epitopes of VGF, specially produced in Prof. G-Luca Ferri laboratory by

immunizing rabbits, sheep, goats, hens or guinea pigs (occasionally rats). To immunize the animals, synthetic peptides corresponding to well selected regions of the VGF primary sequence were used.

TLQP peptides were found in numerous organs, both in endocrine glands and in organs containing endocrine subpopulations. The external area of the median eminence where release factors or hypothalamic inhibitors are secreted, is densely populated with TLQP-immunoreactive neuronal terminal axons, suggesting an involvement of VGF in hypothalamic regulation of the hypophyseal gland (Brancia et al., 2010). TLQP-peptides appear located in secreting somatostatin cells In the rat stomach and pancreas (Cocco et al., 2007), and with gastric enterochromaffin-like (ECL) cells (Brancia et al., 2010). In mouse, TLQP peptides are accumulated in perikarya of celiac ganglia, in pancreatic central islet cells and also in thin beaded nerve fibres of brown adipose tissues, with fewer in WAT (D'Amato et al., 2015). In the adrenal medulla some TLQP peptides appear to be differentially localized in adrenergic cells and C-terminally shortened forms (VGF(604-612): HVLL peptides) to nor-adrenaline cells (D'amato et al., 2008). In Siberian hamster, TLQP-peptides imunoreactivity was found within cortex cholinergic perikarya, in multiple hypothalamic nuclei, including those containing vasopressin, and in pituitary gonadotropic cells (Noli et al., 2015).

Recently, TLQP peptides are also found to be expressed in spinal cord motor neurons, as well as in human fibroblasts and plasma were they were downregulated in SLA (Brancia et al., 2018). In all these organs and cells, chromatography approaches (gel or HPLC) revealed different molecular weight (MW) forms recognised by the TLQP antibody including including peaks compatible with TLQP-62,-42,-30,-21 (Fig. 3). Untill now the only forms with identified biological activities are TLQP-21 and TLQP-62.

Fig. 3) TLQP sequences. The different sequences of the putative TLQP peptides are described

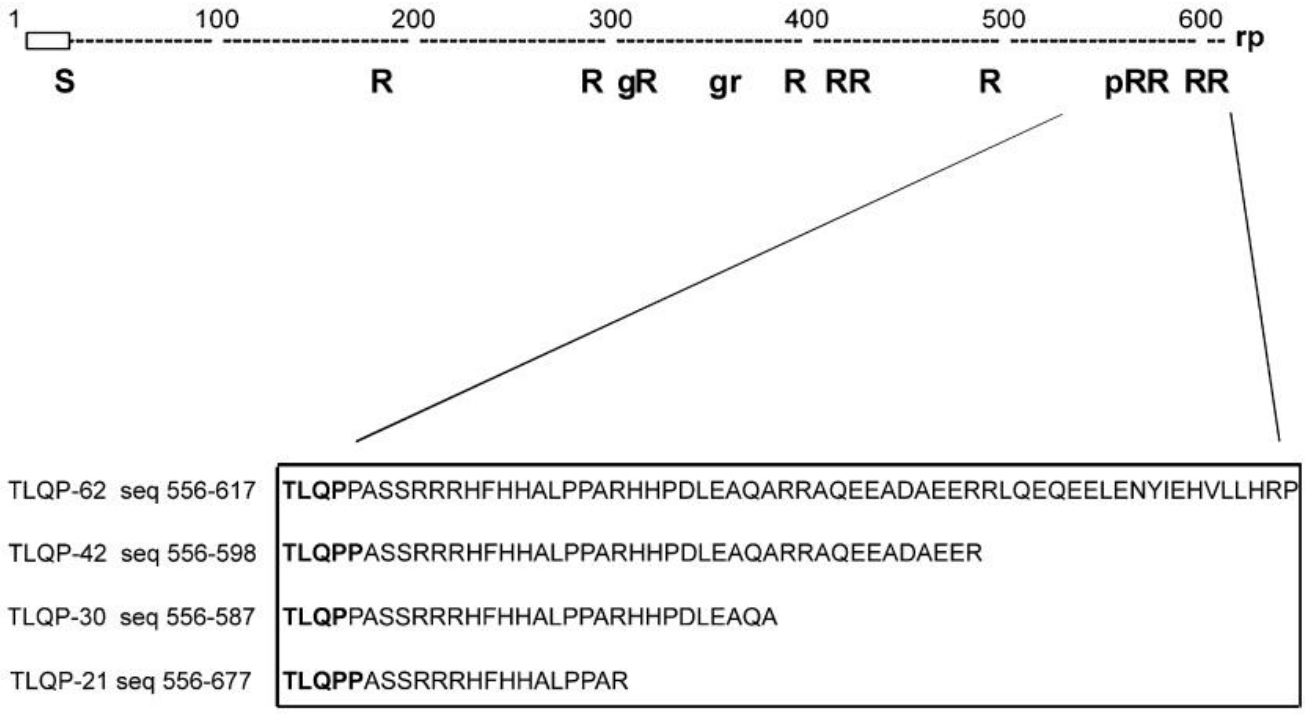

1.5.2 TLQP-21

TLQP-21 is biosynthesized by a region of the VGF precursor close to the C-terminal end of VGF, and was so named because it is composed of 21 amino acids including the sequence "TLQP" (Thr-Leu-Gln-Pro) at its extreme N-terminal. Surprisingly, this peptide injected intracerebroventricular in rats (*i.c.v.*) led to the decrease fat mass associated with increases in serum adrenaline levels, energy consumption and body temperature and prevent obesity induced by the hyperlipidic diet, with no effect on food intake (Bartolomucci et al., 2006; 2009). TLQP-21, not affecting either feeding or hypothalamic peptide mRNAs, but affecting energy expenditure, may function in one such hypothalamic melanocortin 4 receptors (MC4R) regulated extra-hypothalamic sites regulating energy expenditure. In agreement with this hypothesis, has been showed increased catabolic markers in the BAT and WAT following TLQP-21 injection (Bartolomucci et al. 2007). In detail, changes in the BAT were limited to

increased β3-AR expression, and the brown adipocytes specific UCP1 mRNA was up-regulated. On the contrary, molecular analysis of the WAT demonstrated substantial molecular changes: PPAR-δ. Furthermore, PPAR-δ determines fatty acid oxidation and energy uncoupling in WAT (Bartolomucci et al. 2007). TLQP-21 increases lipolysis in murine adipocytes via a mechanism encompassing the activation of noradrenaline / β-adrenergic receptors pathways and dose-dependently decreases adipocytes diameters in two models of obesity (Possenti et al., 2012). TLQP-21 is also biologically active on the muscle of the rat stomach, determining its contraction (Severini et al., 2009), and has been shown to be released from the islets of Langerhans, which suggests that it works through paracrine or autocrine mechanisms (Stephens et al. 2012).

In addition, TLQP-21 showed other numerous biological activities: *in vitro* induces gastric contraction of the fundic zone, mediated by the release of prostaglandins, while following an intracerebroventricular injection, it reduces gastric refilling by about 40% (Severini et al., 2009). Peripheral injections of TLQP-21 lead to hyperalgesia in an inflammatory pain model, while its central administration produces an analgesic effect (Rizzi et al., 2008). More recently, several actions of TLQP-21 have been seen at different levels in the reproductive axis of male rats, in fact the central administration of this peptide induced an acute response through the secretion of the gonadotropin-releasing hormone (GnRH). *In vitro*, the same peptide induces the secretion of luteinizing hormone (LH) in the pituitary gland of male rats at puberty, but not in adults (Pinilla et al., 2011). A study carried out by Severini and collaborators in 2008, demonstrated the dose-dependent antiapoptotic action of TLQP-21 peptide on a subpopulation of cerebellar granule cells, following cell death induced by serum and K^+ deprivation.

The C-terminal internal fragment TLQP-21, has recently been implicated in glucose homeostasis (Stephens et al., 2012). TLQP-21 has been shown to modulate glucose-stimulated insulin secretion (GSIS) and glucose homeostasis and to protect β cells from degeneration in rats (Stephens et al., 2012).

Indeed, TLQP-21 has been shown to be released from the islets of Langerhans, with a possible paracrine or autocrine mechanisms. TLQP-21, as reported previously, did not strongly increase insulin release under the low-glucose condition but did produce a positive effect on GSIS in the INS1E cell line (Stephens et al., 2012).

In the Siberian hamsters (*Phodopus sungorus*), TLQP-21 causes a reduction of food intake, body weight, and mass of white adipose tissue (WAT) imitating a central component of the catabolic state, typical of this species when they are in the "*Short Day*" adaptation phase during the winter period (Jethwa et al. al., 2007; Jethwa and Ebling, 2008).

1.5.3 TLQP-62

The most extensive version of the previous peptide, extended to the extreme C-terminal of VGF, is called **TLQP-62**. It was found to show activity on synaptic plasticity (Alder et al., 2003, Bozdagi et al., 2008, Thakker-Varia et al., 2007), furthermore it was even found to be a potent inducer of insulin secretion in glucose-stimulated insulinoma cell lines, suggesting it could be an endocrine, paracrine and / or autocrine factor with a strong insulinotropic action (Petrocchi-Passeri et al., 2015). TLQP-62 fragment caused strong induction of insulin secretion *in vitro* in the presence of low glucose. This stimulatory effect is dose dependent, and it potentiated glucose-stimulated insulin secretion (GSIS). TLQP-62 also quickly increased intracellular calcium mobilization in pancreatic β-cells, an event dependent on calcium influx from the extracellular compartment as well as from intracellular storage (Lemmens et al. 2001). *In vivo*, administration of TLQP-62 improved glucose tolerance in mice, which suggests that the peptide exerts an insulin secretagogue effect *in vivo* as well. The significant improvement of glucose tolerance was particularly evident at the 30 min time point, which is suggestive of enhanced insulin secretion, despite insulin levels were not directly determined; therefore, further studies are needed to support this conclusion. It was also reported that the action of TLQP-

62 required the presence of a physiological glucose level (4.5 mM), because calcium influx from outside to inside of the cell, is decreased in glucose-free medium (Petrocchi-Passeri et al., 2015).

1.5.4 TLQP peptides in metabolic diseases

The TLQP peptides, appear implicated in metabolic diseases, other than in the control of the energetic balance, including diabetes above all.

In type 1 diabetes, which arises as a consequence of the deterioration of the pancreatic β cells, there is over-expression of the transcription factor Nkx6.1, which increases the replication of β cells and simultaneously induces the secretion of glucose-stimulated insulin (GSIS) (Schisler et al., 2005; Schisler et al., 2008). Subsequent research has shown that the transcription factor Nkx6.1 induces the expression of VGF, and this may be necessary and sufficient to trigger the GSIS mediated by Nkx6.1 (Stephens et al., 2012).

Chronic administration of TLQP-21 in Zucker Diabetic Fatty (ZDF) rats would delay the onset of diabetes by preserving the cellular mass of the pancreatic islets. In addition, in vitro studies have shown that TLQP-21 performs a similar action to exendin 4, blocking apoptosis of β cells (Stephens et al., 2012).

In summary, according to the Stephens group TLQP-21 shows a series of anti-diabetogenic properties including:

- strengthening of the GSIS;
- increase in glycemic control;
- reduction of apoptosis of β cells.

The only study performed so far on alterations of VGF peptides in human diabetes, has shown that plasma of patients with type 2 diabetes outlines an altered profile, with significant reduction of TLQP peptides in subjects with type 2 diabetes (D'Amato et al., 2015).

Furthermore, this study shows that there are not only differences between patients with diabetes of type 2 and the euglycemic individuals, studied but that further differences correlate to the BMI of the patients themselves. (Fig. 4).

Fig. 4) Levels of VGF peptides in human plasma of individuals with type 2 diabetes (T2D) and euglycemic individuals. Levels were measured on normal, overweight and obese individuals, both fasted and 120 minutes after glucose intake (D'Amato et al., 2015)

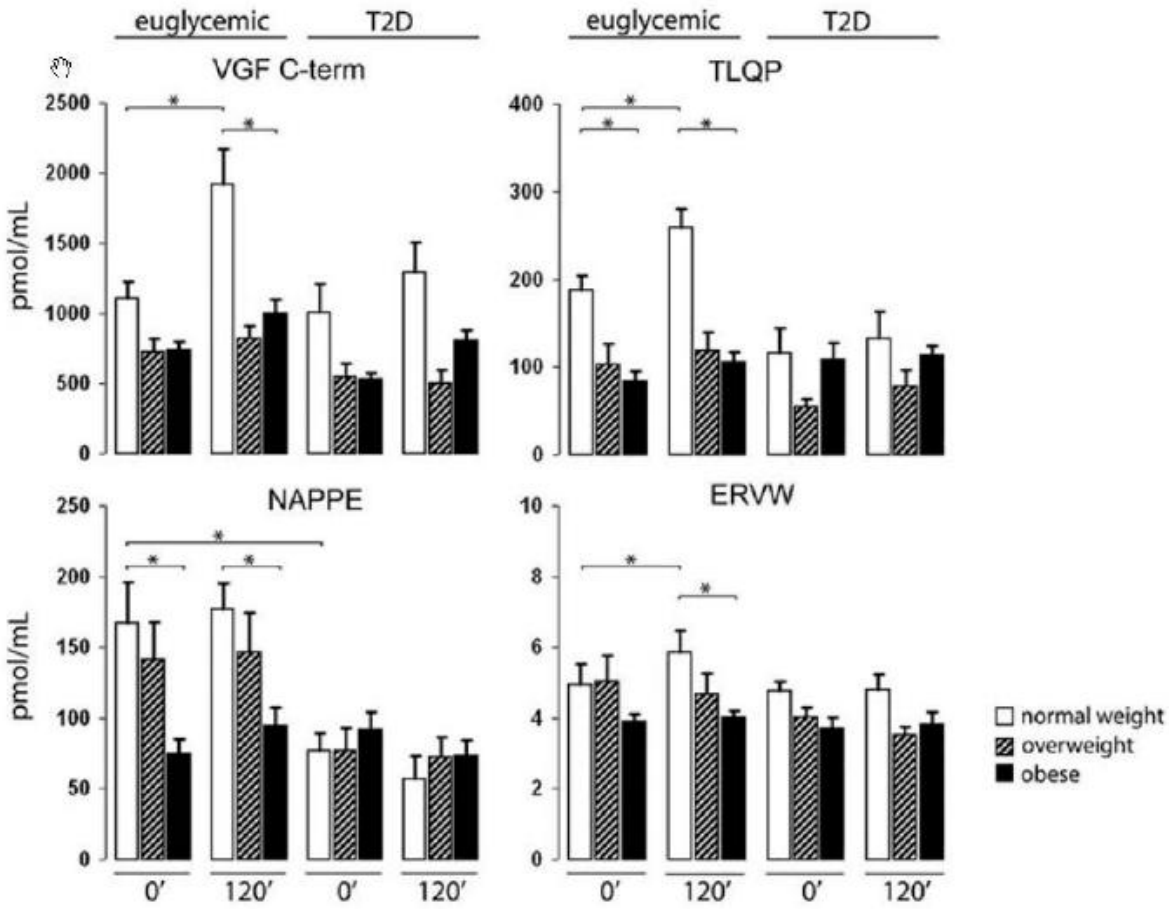

1.6 TLQP Receptors

A first existence of a class of specific receptors binding TLQP, was demonstrated by Possenti in 2012, in the membrane of adipocytes, such receptors appear to be activated by binding with TLQP-21, present in the terminations of W.A.T., and determining a modulatory pro lipolysis effect. In 2013, Chen and collaborators, using macrophage cells, identified by means of mass spectroscopy, the activation of the complement receptor gC1q following treatment with TLQP-21, in which it causes a mechanical hypersensitivity associated with sciatic nerve damage.

In rats, this complement receptor is expressed in microglia cells of the central nervous system and is indispensable for adipogenesis and insulin signaling (review Lewis, 2015).

Recently TLQP-21 has been identified as the natural agonist for the complement 3a receptor 1 (C3aR1) (Hannedouche, et al. 2013). The C3aR1 is a 54 kDa protein member of the G-protein coupled receptor superfamily, whose role in the innate immune response has been well established (Cravedi et al., 2013). However the expression pattern of C3aR1 has suggested that the role of this receptor may be much broader, ranging from promoting stem cell growth (Ducruet et al., 2012; Klos et al., 2009; Matsumoto et al., 2017) to hormone release from pituitary (Francis, et al. 2003).

The relationship between C3aR1, TLQP-21 and energy balance are not well understood, although it was recently suggested that chronic peripheral treatment with TLQP-21 decreases body weight and fat mass in diet induced obese mice by a mechanism involving β-adrenergic and C3aR1 activation (Cero et al., 2017). Interestingly, even the receptor(s) for the others VGF peptides has (have) not yet been identified. Moreover, the C3aR1 antagonist SB290157 did not inhibit the pro-secretory effect of TLQP-62. Hence, it seems that the most C-terminal portion of the peptide is responsible for receptor binding, however, more structural and pharmacological studies are required to determine this conclusively.

2. AIM OF STUDY

The objective of the current study was to determine the peripheral effects of both TLQP-21 and TLQP-62 on energy expenditure and glucose response, in the Siberian hamster which offers a valid model of adiposity, within the two different states (slim or obese) occurring in response to the winter or summer time, respectively. Furthermore, since the relationship between C3aR1, TLQP-21 and energy balance are not well understood, we also aim to further investigate the relationship between C3aR1 and TLQP-21 in this species.

3. MATERIALS AND METHODS

3.1 Animal model (the Siberian hamster)

Seasonal cycles of adiposity and body weight reflecting changes in both food intake and energy expenditure are the norm in the mammals that have evolved in temperate and polar habitats. Innate circannual rhythmicity and direct responses to the annual change in photoperiod combine to ensure that behavior and energy metabolism are regulated in *anticipation* of altered energetic demands such as the energetically costly processes of hibernation, migration, and lactation.

The Siberian hamster, *Phodopus sungorus*, has been used extensively as a robust model of seasonal change in order to investigate energy expenditure, reproductive changes, and adiposity (Ebling, 2015). The Siberian hamster seasonal change is stimulated by changes in the production of melatonin, which increases during the short day (SD; winter) photoperiod and prompts metabolic and physical changes. Upon exposure to SD photoperiods, they reduce their food intake, even with food *ad libitum*, resulting in reduction of their body weight, abdominal fat reserves, and serum leptin levels, and in change of the coat that appears white. Conversely, exposure to long day (LD; summer) photoperiods increases appetite and results in lipogenesis, increased body mass, larger reproductive organs, elevated leptin production and the coat appears dark (Bartness et al., 1989). The changes are so profound that the

hamsters almost look like another animal (Fig. 5). This comprehensive response to photoperiod provides a good model to investigate in metabolism parameters and obesity in animals with naturally high and low serum leptin levels. At the University of Nottingham, the Siberian hamsters were either transferred to SD conditions for 12 weeks (8h light/16h dark, lights off at 11:00 under controlled temperature at 21±1°C) and on a reverse photoperiod with ad libitum access to food, a 19% protein extruded laboratory chow (Teklad 2019, Harlan, UK), and water for 12 weeks or maintained in LD state (8h dark/16h light, lights off at 11:00). Body weight, food intake and pelage score was measured weekly at the end of the light phase.

All animal procedures were approved by the University of Nottingham Animal Welfare and Ethical Review Board and were carried out in accordance with the UK Animals (Scientific Procedures) Act 1986 (project licence PPL 40⁄3604). Females of both Siberian hamsters and mice, aged 3 months, were bread at the University of Nottingham Biological Support Unit (B.S.U.).

Fig. 5) The Siberian hamsters. Left specimen in LD, right specimen in SD

As expected, the exposure to SD significantly reduced body weight and food intake in Siberian hamsters (Figure 6A and 6B, $p < 0.05$). Interestingly, exposure to SD had no effect on meal duration,

however food intake and meal frequency was significantly reduced in SD animals across the night/day cycle (Figure 6 C-E, $p < 0.05$). Furthermore, exposure to SD was associated with the development of a white pelage (Figure 6 F, $p < 0.05$).

Fig. 6 A-F) A; body weight loss express in percentage. B; meal duration express in seconds (sec). C; food intake express in grams (g). E; counts of meal frequency. F; values of pelage score. LD (Long Day state), SD (Short Day state)

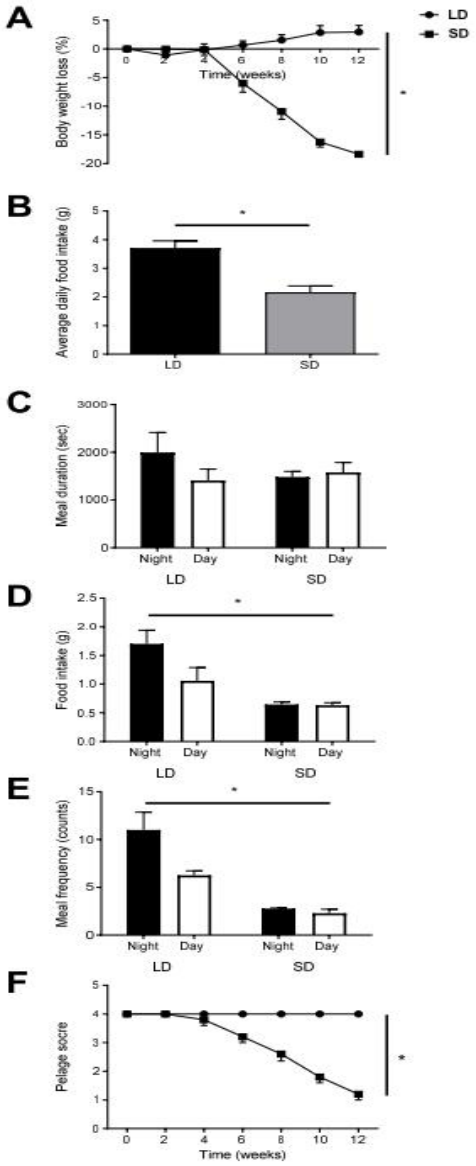

3.2 Injection of TLQP-21 and TLQP-62 for peripheral acute treatment

Animals (female LD Siberian hamsters and mice, of about 3months age) were caloric restricted overnight (i.e. fasted, 16hrs), and received saline, TLQP-62 or TLQP-21 (both 5mg/kg *ip*), followed by saline or glucose injection (at 2g/kg *ip*) after 15 minutes.

Then, after further 15 minutes, blood glucose levels (withdrawn from the left ventricle) were measured through Hemocue Hb 201+ System.

Whole brain, liver, interscapular brown adipose tissue (BAT), interscapular and epididimal white adipose tissue (iWAT and eWAT respectively) and muscle (quad) were collected, snap frozen on dry ice and stored at −80°C until required.

After taking blood from the left ventricle of every animal, each sample was stored in heparinized tubes. The samples were then centrifuged at 10000 rpm for ten minutes and the obtained plasma was taken and stored in clean tubes and stored at -80°C

3.3 TLQP-21 and TLQP-62 peripheral chronic treatments with osmotic minipump

Animals have been surgically prepared (shaved and washed at surgical site); a mid-scapular incision, expanded using a hemostat was made on SD and LD Siberian hamsters (n=8 per treatment per photoperiod), and the s.c. tissue spread to create a pocket to received a subcutaneously implanted Alzet osmotic mini-pump (model 1007D, Charles River) releasing vehicle (saline), TLQP-21 (1mg/kg/day) or TLQP-62 for 7 days as previously described (Lewis, et al. 2017b). Mini-pumps were inserted below the skin on the flank of the Siberian hamster under 1.5% isoflurane anaesthesia. Siberian hamsters were treated with analgesic (5mg/kg s.c., maintained for 3 days with additional fluids, 0.5ml/day, Rimadyl, Pfizer, Kent, UK) and the wound closed with Michel clips. Body weight and food intake were recorded daily, shortly before lights out.

Three days post-surgery animals were transferred to metabolic cages for 48h.

At the end of the seven days, TLQP-62 animals received a i.p. saline or glucose injection (at 2g/kg) and after 30mins blood glucose levels, withdrawn from left ventricle, were measured at 0mins through Hemocue Hb 201+ System and animals were killed.

Whole brain, liver, interscapular brown adipose tissue (BAT), interscapular and epididimal white adipose (iWAT and eWAT respectively) and muscle (quad) were collected, snap frozen on dry ice and stored at −80°C until required.

3.4 Metabolic gases and feeding behavior

After 3 days of TLQP peptides administration, animals were concurrently analysed for multiple respiratory and feeding behaviour parameters using a modified open-circuit calorimeter know as Comprehensive Lab Animal Monitoring System (CLAMS: Linton Instrumentation, Linton, UK, and Columbus Instruments, Columbus, OH, USA). This open-circuit calorimeter is configured for Siberian hamsters with eight mouse chambers, where the hamsters were individually housed with food hoppers (chow was ground down into a rough powder) in the centre of each cage, and dropper-style water bottles. Metabolic parameters to be measured included oxygen consumption (VO_2) and CO_2 production (VCO_2) that allow to calculate respiratory exchange ratio (RER) could be calculated. Locomotor activity was also measured using two sets of infrared beams traversing each cage which measured linear and vertical movement. The system was operated with an air intake of 0.6 Litres/min for each chamber, and an extracted outflow of 0.4 Litres/min. All measurements were taken at room temperature of 21–22°C.

3.5 Immunohistochemistry

To evaluate the expression of C3aR1 in aged-matched female LD and SD *Siberian hamsters* (n=6 per photoperiod), immunoistochemistry (IHC) was perfomed. using standard immunofluorescence techniques.

Animals received an *i.p.* injection of sodium pentobarbitone and then were transcardially perfused with 0.01M PBS (pH 7.2) for 3 minutes followed by 4% paraformaldehyde in 0.1M phosphate buffer saline (pH 7.2) for 5 minutes. The brains were removed, post-fixed for 2 hours and transferred to PBS for storage. Brains were cryopreserved for 24h in 20% sucrose prior to being sectioned using the freezing microtome (60µm coronal sections). Primary antibody (rabbit polyclonal anti-C3aR1), diluted 1:100 (abcam, ab140777) was incubated on brain sections for 48 hours at +4°C. After washing, the sections were incubated with biotinylated goat anti-rabbit, diluted 1:400 (VectorLabs, BA-1000) for 1 hour at room temperature and then washed. The sections were then incubated with the tertiary antibody, avidin fluorescein D, diluted at 1:200 (Vectorlabs, A- 2001) for a further hour at room temperature. After washing, sections were mounted on to APES coated slides, dried and cover slipped with DABCO fluorescent mounting media. Images were captured using a Nikon Optiphot-2 fluorescent microscope and SPOT software. Fluorescent quantification within the tanycyte layer was completed by researchers blind to photoperiod conditions. Areas of fluorescence and relative fluorescence intensity for brain regions were quantified using NIH ImageJ software as previously described (Schneider, et al. 2012). Background was normalised across sections to ensure that intensity was measured equally across photoperiods. Intensity measures captured across ependymal cell layer and averaged across each animal for C3aR1 to be compared across photoperiods as mean fluorescent intensity.

3.6 Western Bloting Analysis

For WB analysis of TLQP-21 receptor, tissues were first homogenated, the proteins extracted and quantified, then the samples were run and the signals were analysed by a dedicated software.

3.6.1 Protein extraction process

Tissue chunk (≅ 30 – 50 mg of wet tissue) was put in a clean vial, and 4 μl of protease inhibitors cocktail (SIGMA P-8340) was added for every ml of buffer (50 mM HEPES from SIGMA H4043, 10% Glicerol from SIGMA G8773; 1 mM EDTA from SIGMA E4884; 10 mM NaF from SIGMA S6521; 1 mM Na_3VO_4 from SIGMA S6508 taking 5ml of 100mM activated solution or 2.86 ml of 175 mM; 150 mM NaCl; 1% TRITON x-100 from SIGMA x-100; pH: 7.5).

6 times dilution (i.e. 50 mg of tissue in 300 μl buffer plus protease inhibitors) was generally applied, while a 10 times dilution was used for small amounts of tissue (≅ 10 – 20 mg).

Homogenisation was made with polytron at medium speed (2-3) for 30 seconds on ice, and leaved on ice for 20 minutes and then transfered to eppendorf tube and spin at 10.000g for 20 minutes at 4°C.

Supernatant was transfered to clean eppendorf, and then 5 μl was transfered into a separate eppendorf tube containing 45 μl of distilled water (diluition 1:10) and stored at –20°C (Stable for weeks).

3.6.2 Protein quantification

The preparation of diluted albumin (BSA) standards for protein quantification (BCA Protein Assay Kit, Thermoscientific 23225) is described in Table 1.

Table 1. Preparation of Diluted Albumin (BSA) Standards

Dilution Scheme for Standard Test Tube Protocol and Microplate Procedure (Working Range = 20-2,000µg/mL)			
Vial	**Volume of Diluent (µL)**	**Volume and Source of BSA (µL)**	**Final BSA Concentration (µg/mL)**
A	0	300 of Stock	2000
B	125	375 of Stock	1500
C	325	325 of Stock	1000
D	175	175 of vial B dilution	750
E	325	325 of vial C dilution	500
F	325	325 of vial E dilution	250
G	325	325 of vial F dilution	125
H	400	100 of vial G dilution	25
I	400	0	0 = Blank

10µL of each standard or unknown sample replicate was pipetted into a microplate well (working range = 125-2000µg/mL) followed by 200µL of the working reagent (obtained by mixing 50 parts of BCA Reagent A (containing sodium carbonate, sodium bicarbonate, bicinchoninic acid and sodium tartrate in 0.1M sodium hidroxide) with 1 part of BCA Reagent B (containing 4% cupric sulfate) (50:1, Reagent A:B), then plate was mixed thoroughly on a plate shaker for 30 seconds, covered and incubated at 37°C for 30 minutes.

The absorbance was measured at or near 562nm, on a spectrophotometer plate reader.

The average 562nm absorbance measurement of the blank standard replicates was subtracted from the 562nm measurements of all individual standards and unknown sample replicates.

A standard curve was prepared by plotting the average blank-corrected 562nm measurement for each BSA standard vs. its concentration in µg/mL.

Based on the newly obtained protein concentration, the volume of protein extract was determined to ensure exactly 50 µg in each well of the gel.

3.6.3 Western Blot loading

Samples containing 50 μg of protein was mixed with loading buffer (2x SDS) and heated at 95◦C for 5 mins, and loaded on to a 10% polyacrylamide gel on 100 volts for 90 minutes and transferred electrophoretically to nitrocellulose membranes, then blocked for 20 minutes with milk powder in TBS-T (Tris buffer + 10 % Tween-20).

Membranes were probed with a 1:1000 dilution of rabbit monoclonal anti C3aR1 and of mouse monoclonal anti Actin (Abcam, Cambridge, MA) antibodies overnight at 4◦C, followed by incubation with secondary goat-anti rabbit and goat-anti mouse HRP-linked antibody (1:2000) for 1 hour at room temperature.

Detection of membranes was performed scanning with LiCor Odyssey 9120 Imaging System.

3.6.4 Analysis of the WB signal

To evaluate the signal strength of the proteins (TLQP-21 receptor) expressed in Western Blots, the AIDA system was used. The software based on how much each area was more o less intense and extended, calculated exactly the intensity of colouring pixels for each area taken into consideration, attributing an arbitrary numerical value based on how much each area was more or less intense and extended. Another area of the same size that surrounds each signal, was made in a clean part of the WB, a background, in order that the system subtracts from each signal area, the background value of the clean gel. This procedure was performed for every single band that appears in the WBs.

Supposing that the actin expression (a structural protein of cytoskeleton) does not change related to treatments or photoperiodicity, once each numerical value has been obtained for every band of each sample. The values of actin expression was averaged as control in order to normalize the procedure, then a ratio between each value of the signal intensity of C3aR1 and the average of actin was

calculated. This ratio gaves the final value for every sample analyzed, and then an average of the ratios of all the animals in SD, in LD and treated with TLQP-21 or saline.

3.7 ELISA test for insulin measurement

Sandwich ELISA was performed according to manual protocol of the rat / mouse insulin ELISA Kit (Cat. # EZRMI-13K from Millipore) based on the following steps:

1) Insulin within the samples was captured to the wells of a microtiter plate coated by pre-titered amount of a monoclonal mouse anti-rat insulin antibodies incubate at room temperature for 2 hours on a orbital microtiter plate shaker set to rotate at moderate speed (about 400 to 500 rpm), and then the biotinylated polyclonal antibody was used to bind the captured insulin (with moderate shaking at room temperature for 30 min on the microtiter plate shaker).

2) unbound materials from samples were washed away with distilled water,

3) horseradish peroxidase antibody was used to the immobilizer bind biotinylated antibodies,

4) free enzyme conjugates were washed away

5) immobilized antibody-enzyme conjugates with horseradish peroxidise was quantificated by using the substrate 3,3',5,5'-tetramethylbenzidine.

The enzyme activity was measured spectrophotometrically by the increased absorbency at 450 nm, corrected from the absorbency at 590nm, after acidification of formed products. Since the increase in absorbency is directly proportional to the amount of captured insulin in the unknown sample, the latter can be derived by interpolation from a reference curve generated in the same assay with reference standards of known concentrations of insulin.

3.8 Statistical analysis

Descriptive statistics (mean ± S.E.M.) were generated using Graphpad Prism (Prism 6.0, GraphPad, San Diego, CA, USA). After checking for normality of distribution and equality of variance, body weight, food intake and CLAMS data were analysed using a two-way (treatment × sampling time) repeated measures ANOVA, with Bonferroni corrected post-hoc t-tests when a significant main effect or interaction was detected. Data were analysed by Student's unpaired t-test.

No animals were excluded from the analysis. Statistical significance was declared at $p<0.05$

4. RESULTS

4.1 Chronic peripheral effects of TLQP-21 in Siberian hamsters

The chronic peripheral effects of TLQP-21 on female Siberian hamsters metabolism in SD and LD states, was evaluated (thanks to Prof.ssa Cristina Cocco who did the first pilot experiments).

4.1.1. TLQP-21 in SD Siberian hamsters

In the SD state, TLQP-21 reduced cumulative food intake ($p < 0.03$), as a consequence of reduced meal duration in the dark phase ($p < 0.05$; Fig. 7 A-C), increased energy expenditure ($p < 0.04$; Fig. 8 A-C), and significantly reduced body weight ($p < 0.04$; Fig. 9 A-C).

Fig. 7 A-C) Average daily (3 days) meal duration (A), food intake (B), and meal frequency (C) of SD female Siberian hamsters treated with TLQP-21 versus saline treated controls. Chronic peripheral treatment with TLQP-21 reduces food intake in female SD Siberian hamsters exposed to SD for 12 weeks; as a consequence of reduced meal duration. Values are group mean ± SEM, n = 8 per group, * p < 0.05

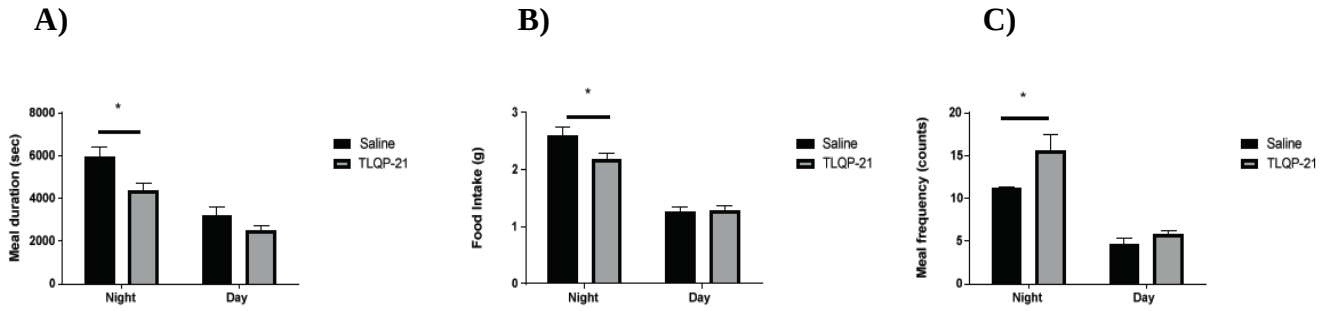

Fig. 8 A-C) Average daily (3 days) VO2 consumption (A), carbon dioxide production (B), energy expenditure (C), in female Siberian hamsters exposed to SD for 12 weeks. The black and white bands above every figure indicate the dark and light phase, respectively. TLQP-21 exposure increases oxygen consumption, carbon dioxide production, and energy expenditure in female SD Siberian hamsters. Values are group mean ± SEM, n= 8 per group; * p < 0.04

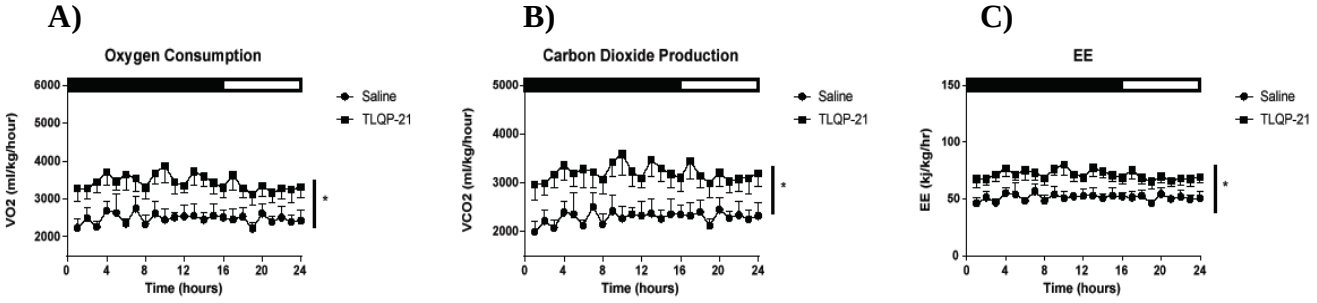

Fig. 9 A-C) Average of measurements (hours) within 7 days for body weight (A) and cumulative food intake (B), while ambulatory activity (C) was measured as the average of the number of beam breaks within the day. The black and white bands in figure C indicate the dark and light phase, respectively; TLQP-21 significantly reduced body weight, and cumulative food intake while activity was not affected * p < 0.04

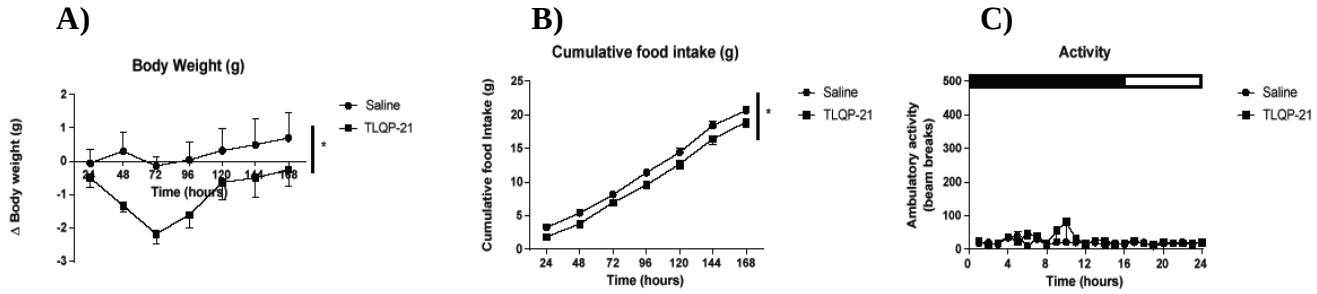

4.1.2. TLQP-21 in LD Siberian hamsters

In LD – obese animals, the chronic peripheral treatment with TLQP-21 (1mg/kg/d for 7 days), does not generate any significant effect for each of the parameters that we have seen in the SD (see Fig. 10-12).

Fig. 10 A-C) Average daily (3 days) meal duration (A), food intake (B), and meal frequency (C) of LD female Siberian hamsters treated with TLQP-21 versus saline treated controls. Peripheral treatment with TLQP-21 does not reduces food intake in female LD Siberian hamsters

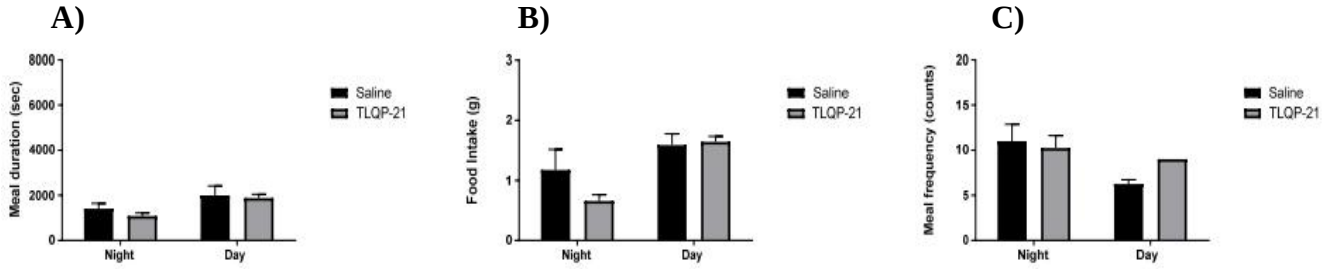

Fig. 11 A-C) Average daily (3 days) VO2 consumption (A), carbon dioxide production (B), energy expenditure (C), in LD female Siberian hamsters. The black and white bands above every figure indicate the dark and light phase, respectively. TLQP-21 exposure does not increases oxygen consumption, carbon dioxide production, and energy expenditure in female Siberian hamsters.

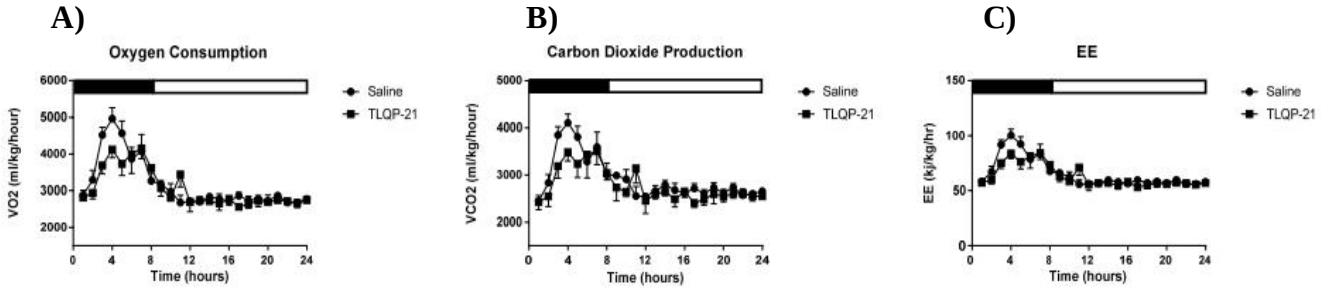

Fig. 12 A-C) Average of measurements (hours) within the 7 Days for body weight (A) and cumulative food intake (B), while ambulatory activity (C) was measured as the average of the number of beam breaks within the day. The black and white bands in figure C indicate the dark and light phase, respectively. TLQP-21 does not affect body weigh, cumulative food intake and activity in LD Siberian Hamsters

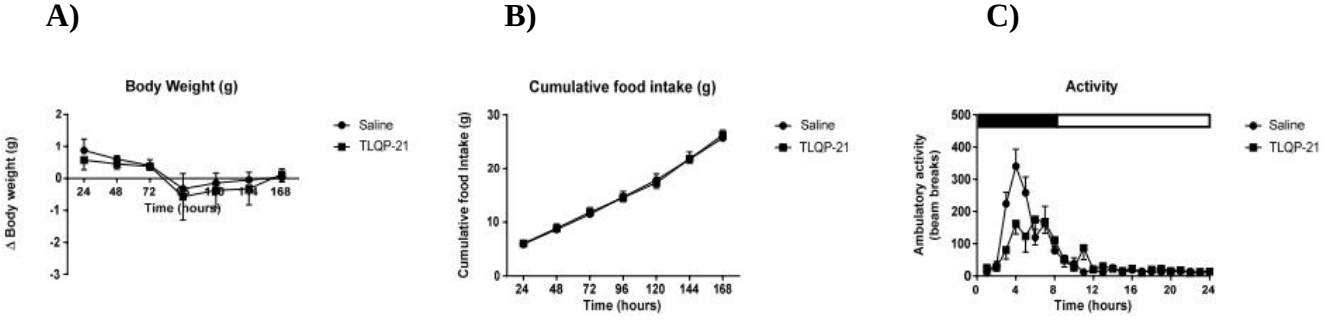

4.2 C3aR1 expression in Siberian hamsters

We evaluated the changes in the expression of the TLQP-21 receptor (C3aR1) in tissues from either TLQP-21 treated and naive (in both SD and LD Siberian hamsters).

4.2.1 Expression of the C3aR1 in hypothalamus

Significant reduction of the C3aR1 expression was seen in the entire hypotalamus of all SD Siberian hamsters irrespectively of the TLQP-21 chronic treatment (Fig. 13, $p < 0.03$) compared to the hamsters in the LD state.

Indeed no significant difference in the C3aR1 expression was found in the animals treated with TLQP-21 *vs* saline. To confirm this results, the experiment was repeated using drug naïve SD and LD Siberian hamsters, ensuring that the C3aR1 expression still found decreased in SD *vs* LD animals (Fig. 14). Western blotting revealed that the TLQP-21 receptor C3aR1 was significantly reduced in SD animals (LD = 0.37 ± 0.05, SD = 0.27 ± 0.01, 26.6% decrease).

Fig. 13) WB analysis of Anti-C3aR (Red), Anti-Actin (Green)

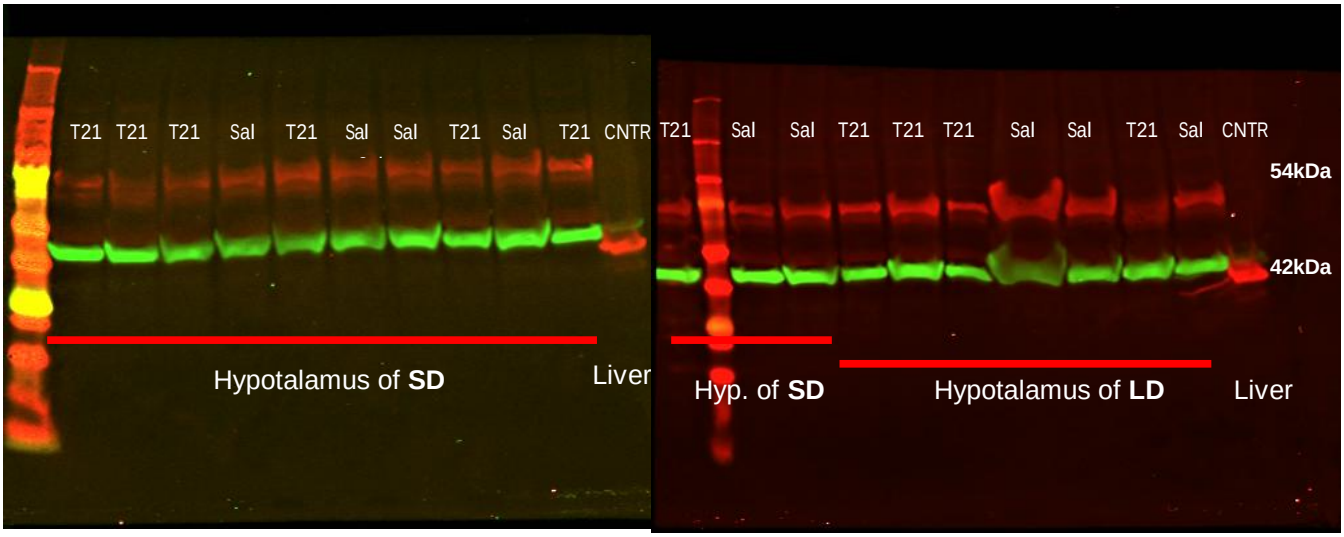

Fig. 14) WB analysis of Anti-C3aR (Red), Anti-Actin (Green); Naive groups

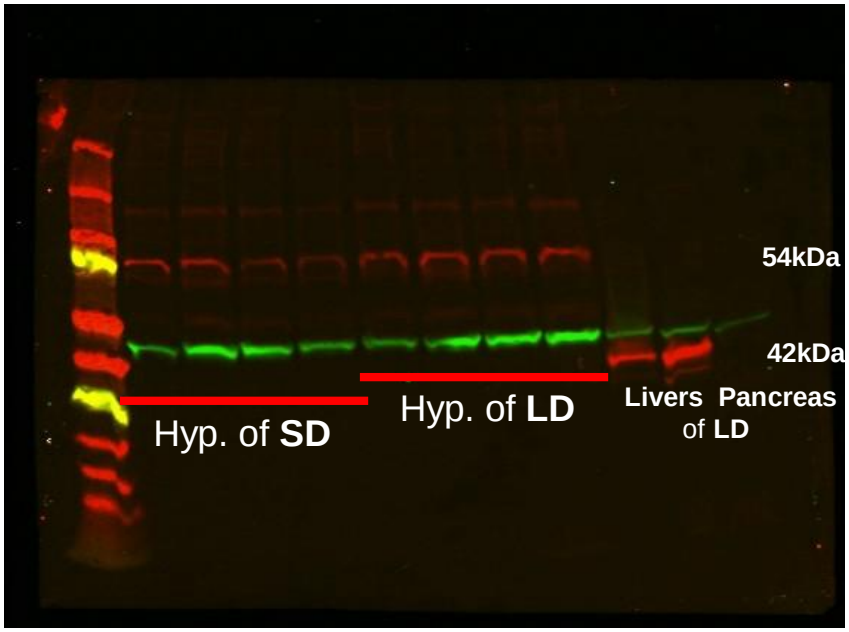

-Fig. 13 and 14:
(LD = 0.37 ± 0.05, SD = 0.27 ± 0.01, 26.6% decrease)
The only significative difference of C3Ar expression is between SD vs LD saline treated animals (p < 0.03) By AIDA (Advanced Image Data Analyzer)

4.2.2 Expression of C3aR1 in tanycytes

Using drug naïve animals, IHC analysis revealed that C3aR1 expression was significantly increased in 3rd ventricle tanycytes in SD Siberian hamsters (LD = 23.95 ± 1.53, SD = 35.97 ± 2.89, 33.4% increase) (Figure 15 A and B).

Fig. 15 A-B) Analysis of fluorescence intensity revealed increased C3aR1 expression in 3rd ventricle tanycytes in SD Siberian hamsters (A).
(B) representative images of the C3aR1 expression in tanycytes of LD and SD animals.
Values are group mean ± SEM, n = 6 per photoperiod, * p < 0.05

A)

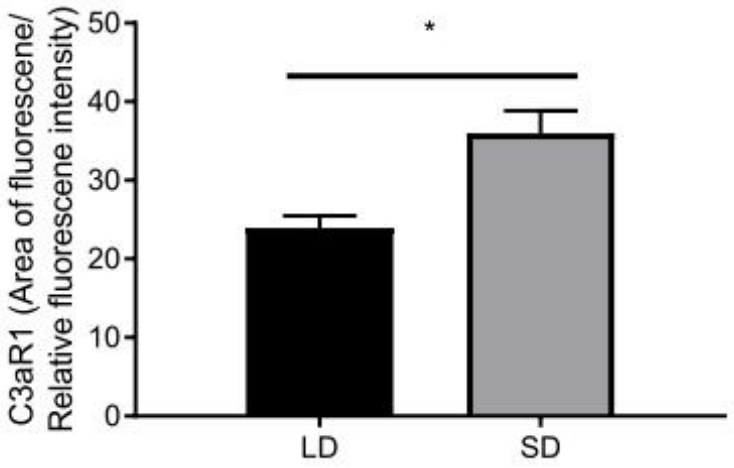

B)

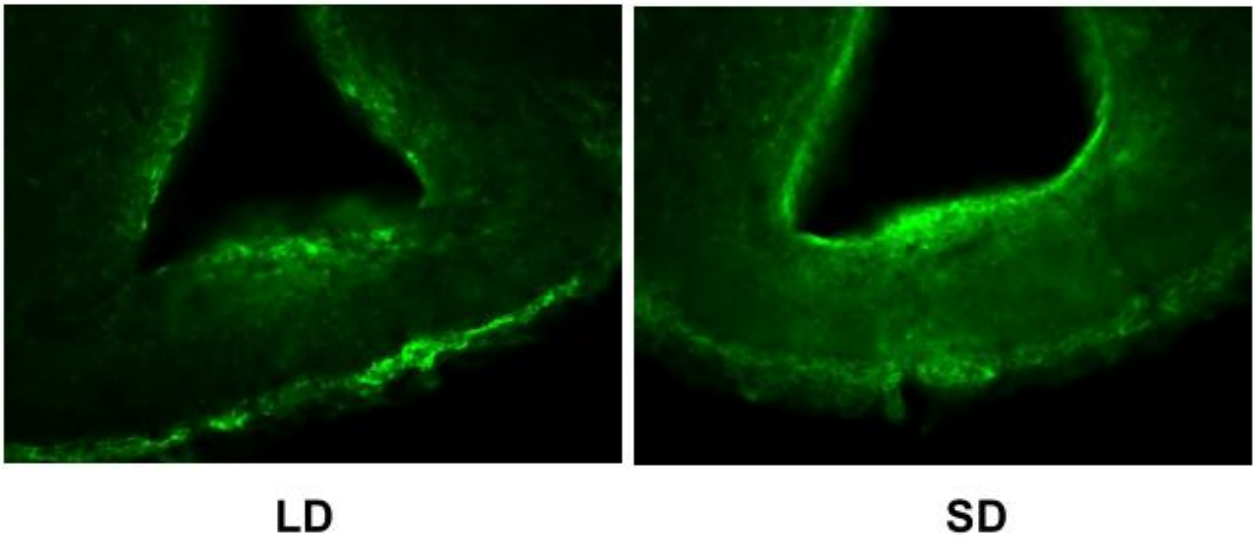

4.2.3 Expression of C3aR1 in liver

In liver of naive SD and LD Siberian hamsters expression of C3aR1 did not change. Interestingly, C3aR1 in liver always appears at 41 kDa size, and not at 54 kDa, as it should be (Fig. 16; see also previous photos of hypotalamus where the liver is used as a control), **suggesting alternative forms of C3aR1 in liver.**

Fig. 16) Livers; WB analysis of Anti-C3aR (Red)

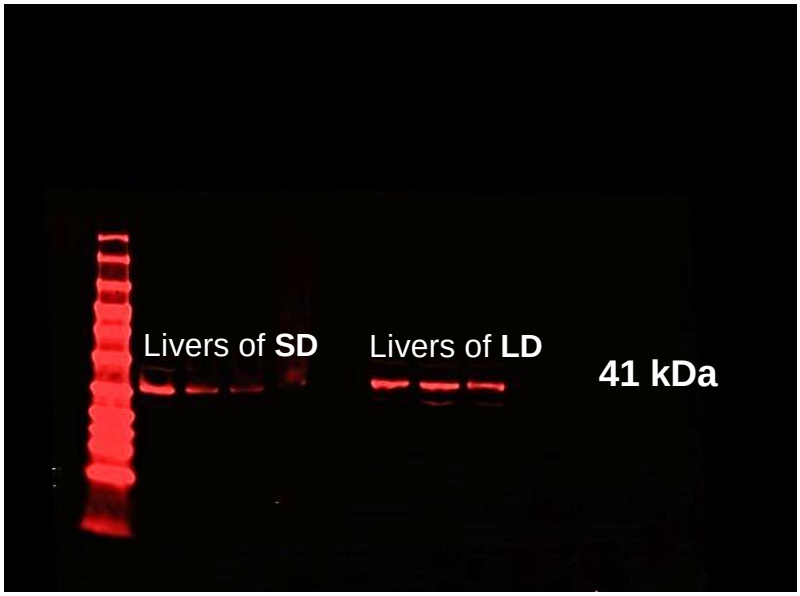

4.2.4 Expression of C3aR1 in pancreatic Langherans islets

In both LD and SD drug naive Siberian hamster, there is not signal of C3aR1 expression (Fig. 17).

Fig. 17) WB analysis of Anti-C3aR (Red), Anti-Actin (Green). Expression of C3aR1 is detectable in hypotalamus and liver (controls) but not in pancreatic islets. Actin was use to normalized the samples

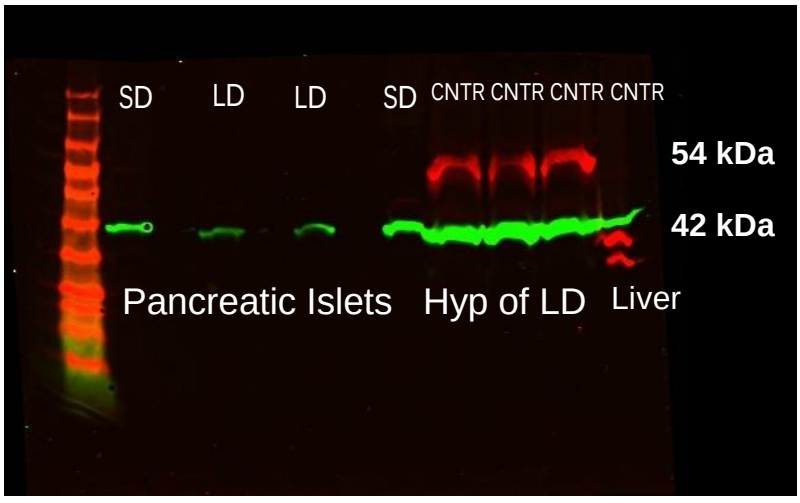

4.2.5 Expression of C3aR1 in adipose tissues

In both white (eWAT Fig. 18 and iWAT Fig 19) and brown (BAT Fig. 20) adipose tissues of LD and SD saline treated Siberian hamsters, no C3aR1 detectable a mount was evident in Western Blot.

Fig. 18) WB analysis of Anti-Actin (Green)

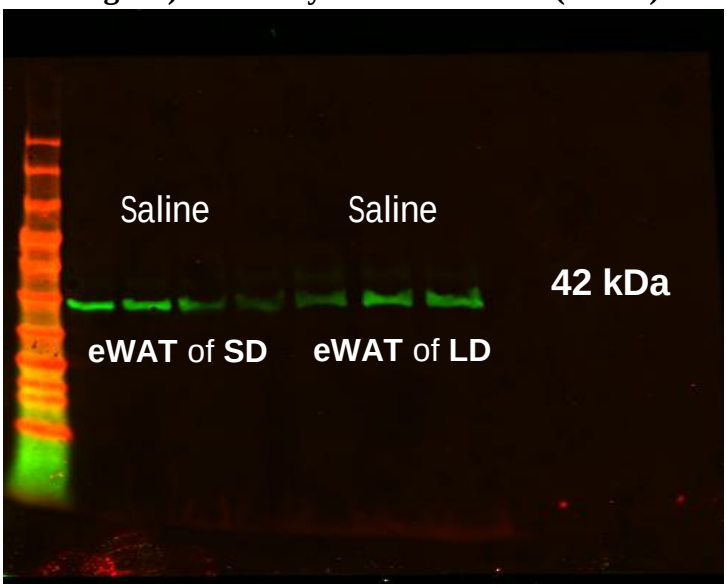

Fig. 19) WB analysis of Anti-Actin (Green)

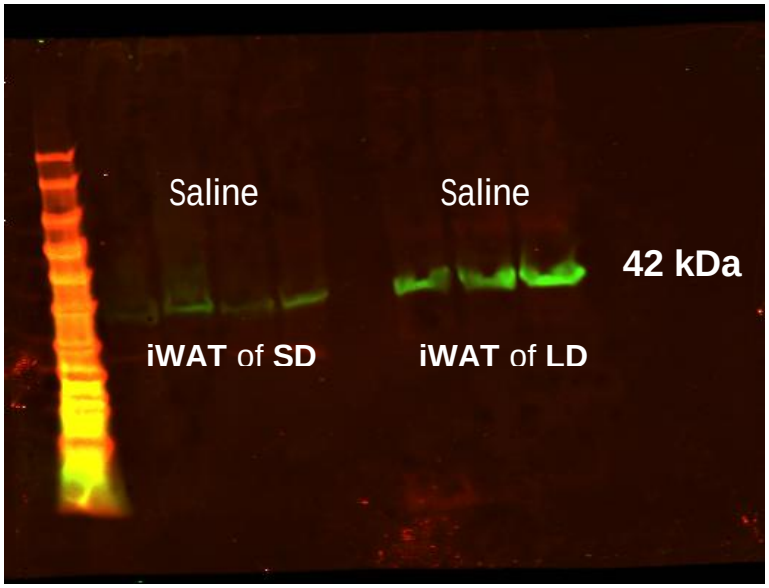

Fig. 20) WB analysis of Anti-Actin (Green)

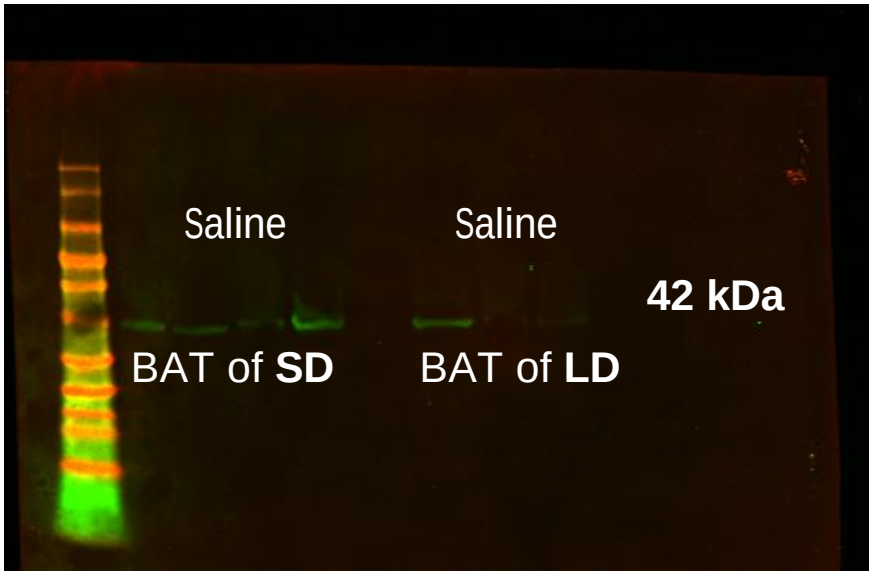

4.3 Metabolic effects of chronic peripheral TLQP-62 administration in Siberian hamster

In both SD and LD animals the chronic treatment with TLQP-62 does not generate any significant effect for each of the parameters measured trough CLAMS (Fig. 21, 22, 23 shows representative results in SD animals).

Fig. 21) The abscissa expressed the total time spend inside the CLAMS hours, while ordinates indicate the Oxygen consumption (ml/kg/hour), expressed as the average of all animals of the two groups (Blue is saline group, orange is TLQP-62 group). No significant differences were revealed

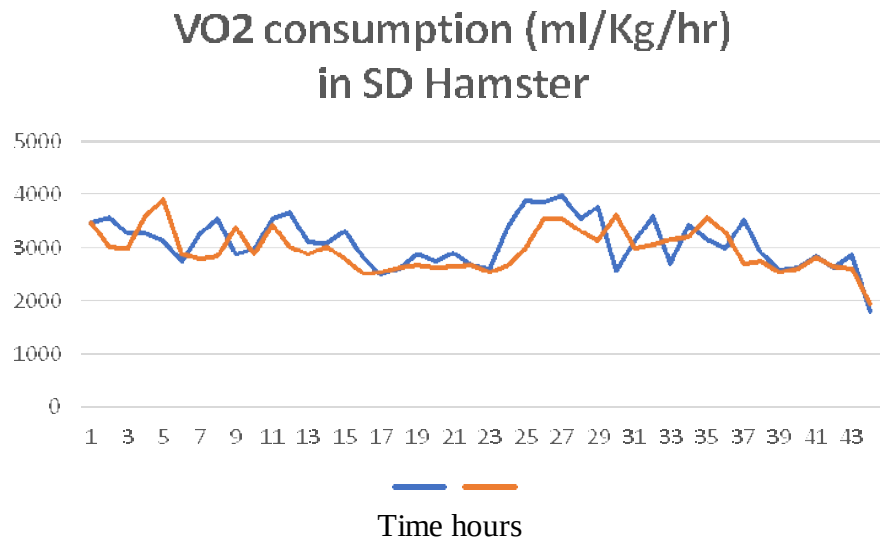

Fig. 22) The abscissa expressed the total time spend inside the CLAMS (hours), while the ordinates indicate the Carbon Dioxide production (ml/kg/hour), expressed as the average of all animals of the two groups (Blue is saline group, orange is TLQP-62 group). No significant differences were revealed

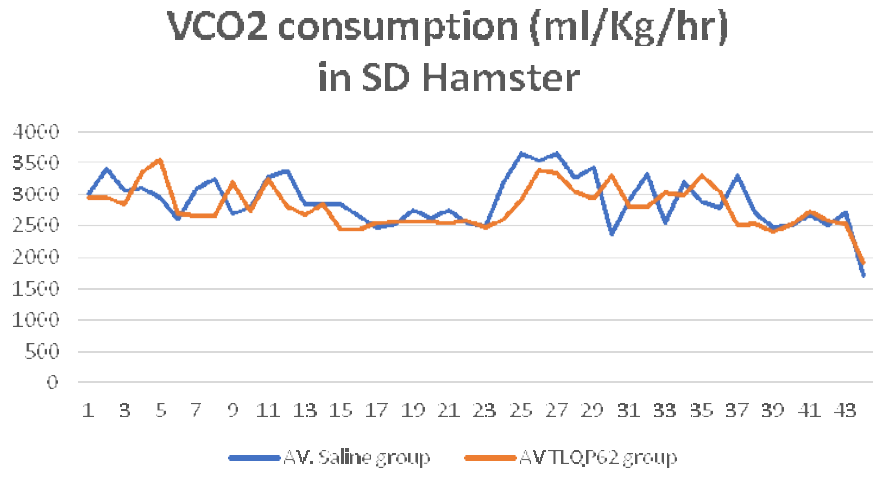

Fig. 23) The abscissa expressed the total time spend inside the CLAMS (hours), while the ordinates indicate the Energy Expenditure (kJ/Kg/hr), expressed as the average of all animals of the two groups (Blue is saline group, orange is TLQP-62 group). No significant differences were revealed

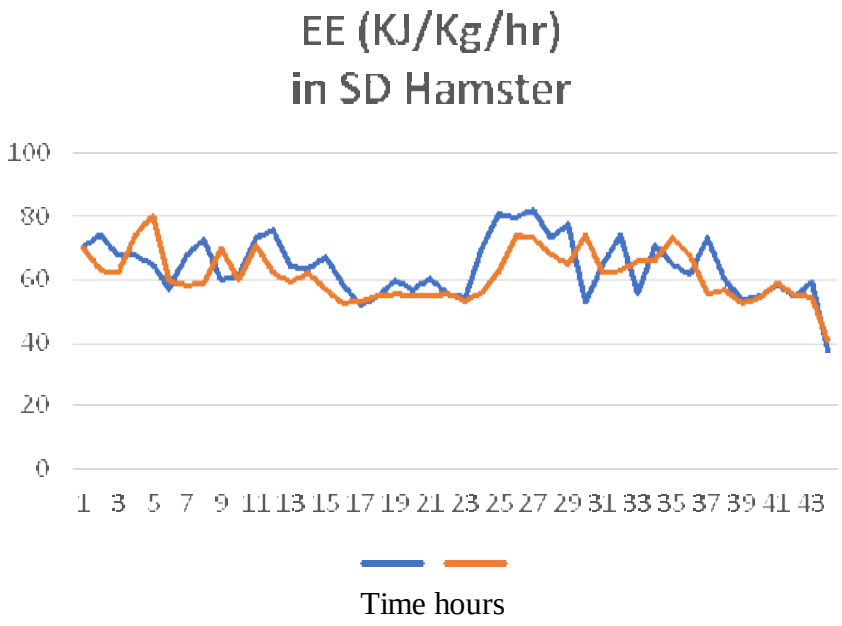

as far as food intake and body weight are concerned, we did not show the data because even in these parameters there were not any variations.

4.4 Blood glucose effects of chronic peripheral TLQP-62 administration in Siberian hamster

4.4.1 TLQP-62 reduced blood glucose level in SD Siberian hamster

After 30 minutes from *i.p*. glucose injection in SD slim animals, TLQP-62 chronic treatment significantly reduced blood glucose level compared to saline (SD: glucose levels: 15.2 mMol/l *vs* 8.7 mMol/l; saline *vs.* treated animals, respectively; $p < 0.05$, Fig. 24).

Fig. 24) Effect of TLQP-62 *Chronic* administration on glycemia in SD Siberian hamsters. Average blood glucose levels in saline animals is: 15.2 mMol/l *vs* 8.7 mMol/l of treated animals; *p < 0.05

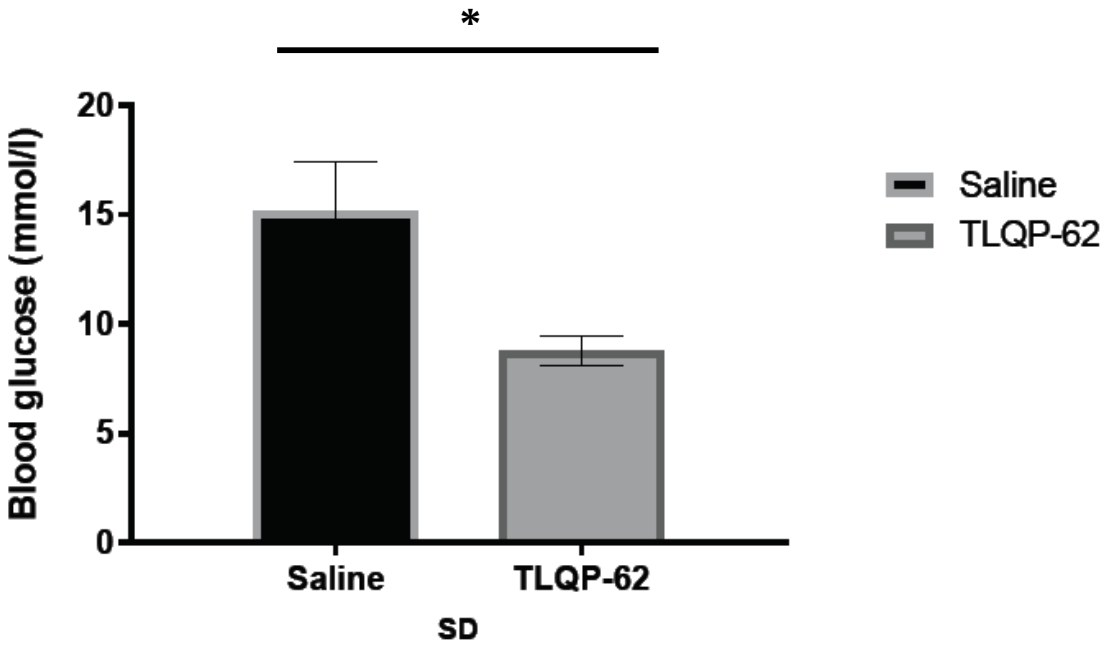

4.4.2 TLQP-62 reduced blood glucose level in LD Siberian hamster

After 30 minutes from *i.p*. glucose injection in LD obese animals, TLQP-62 chronic treatment significantly reduced blood glucose level compared to saline (LD: blood glucose levels: 8.2 mMol/l *vs.* 6.75 mMol/l, saline *vs* treated animals, respectively; $p < 0.05$, Fig. 25).

Fig. 25) Effect of TLQP-62 *Chronic* administration on glycemia in LD Siberian hamsters. Average blood glucose levels in saline animals is: 8.2 mMol/l *vs* 6.75 mMol/l of treated animals; *p < 0.05

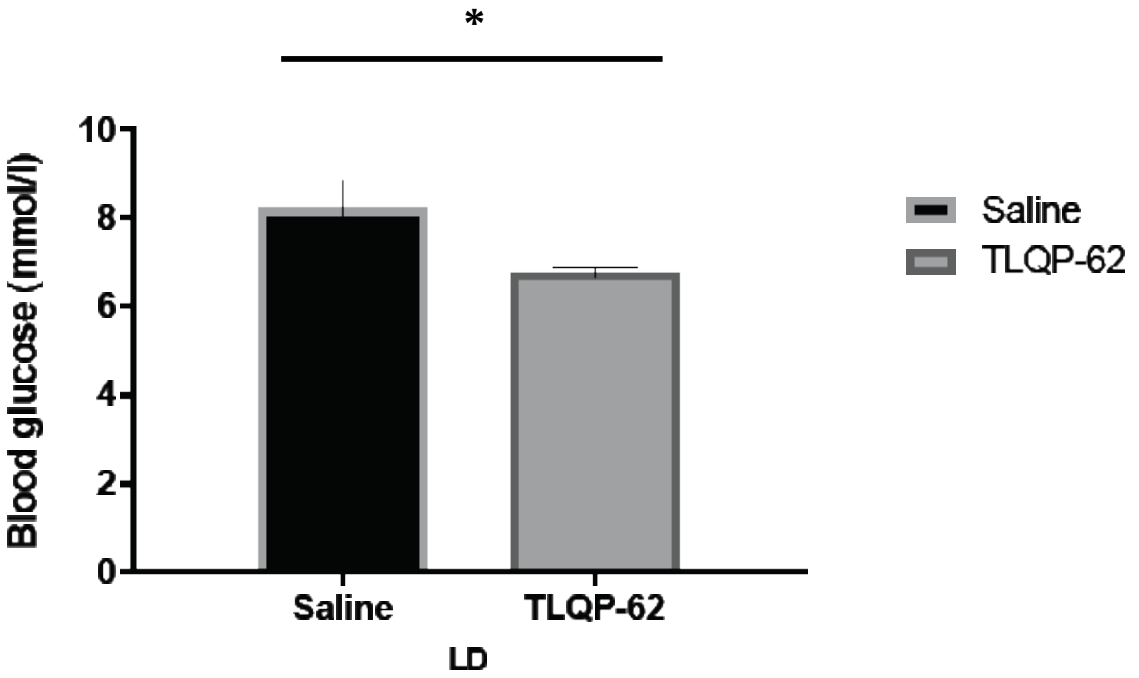

4.5 Blood glucose effects of TLQP-62 acute treatment in LD Siberian hamster

In order to confirm the TLQP-62 effect on decreasing glycemia, the acute administration was also investigated in LD Siberian hamsters.

It has to be noted here that, in these animals, the blood was collected after 15 minutes from the glucose administration, because we previously revealed that in LD saline treated animals, the blood glucose values are elevated after 15 minutes but decreased after 30 minutes, contrary to what occurs in saline treated SD animals in which the blood glucose levels were instead very high after 30 minutes from the glucose administration.

Indeed after 15 minutes from *i.p.* glucose injection in LD obese animals TLQP-62 acute treatment significantly reduced blood glucose level compared to saline (blood glucose levels: 19.9 mMol/l *vs.* 14.25 mMol/l, saline *vs.* treated animals, respectively; (See fig. 26, $p < 0,05$).

Fig. 26) On the abscissa are expressed the animal groups used for the GTT (Glucose Tollerance Test), while in ordinates are expressed (mMol/l) the blod glucose levels.
Average blood glucose levels: 19.9 *vs* 14.25 mMol/l; saline *vs.* treated animals respectively, *p < 0.05

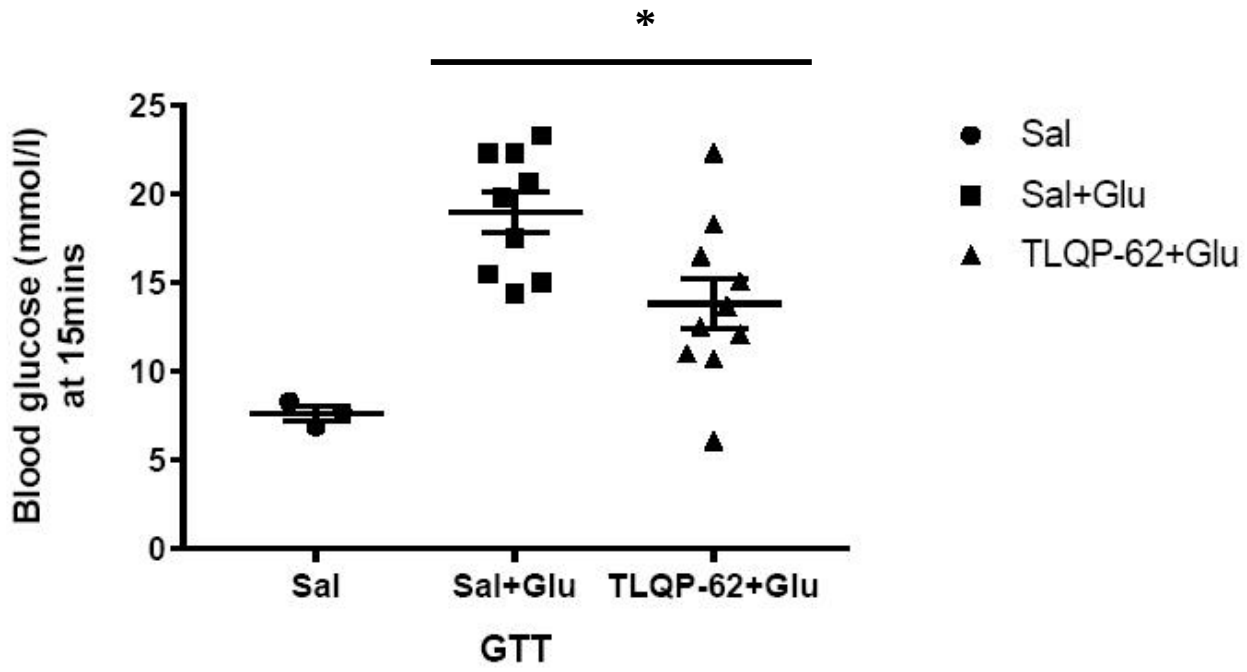

Peripheral administration of TLQP-62 also induces a very strong release of insulin (measured by ELISA) into the blood, compared to controls. However, the OD values of insulin in the blood of the TLQP-62 treated animals was very high and unfortunately out of the range of the standard curve.

4.6 Blood glucose effects of TLQP-62 and TLQP-21 acute treatments in mouse

4.6.1 Effect of TLQP-62 and TLQP-21 on glucose levels.

Administration of TLQP-62 is significantly active in lowering blood sugar levels, fifteen minutes after the glucose load, compared to the saline treated animals ($p < 0.03$). Instead the administration of TLQP-21 has no effect on lowering blood sugar, the values of which are comparable to animals that received saline ($p > 0.05$) (Fig. 27).

Fig. 27) On the abscissa are expressed the groups used for the GTT (Glucose Tollerance Test), in ordinates are expressed (mMol/l) the blood glucose levels.
***p: 0.024988 Sal/Glu *vs* TLQP-62/Glu; *p: 0.000505 Sal/Glu *vs* Sal/Sal; p: 0.82354 Sal/Glu *vs* TLQP-21/Glu (Not Significant)**

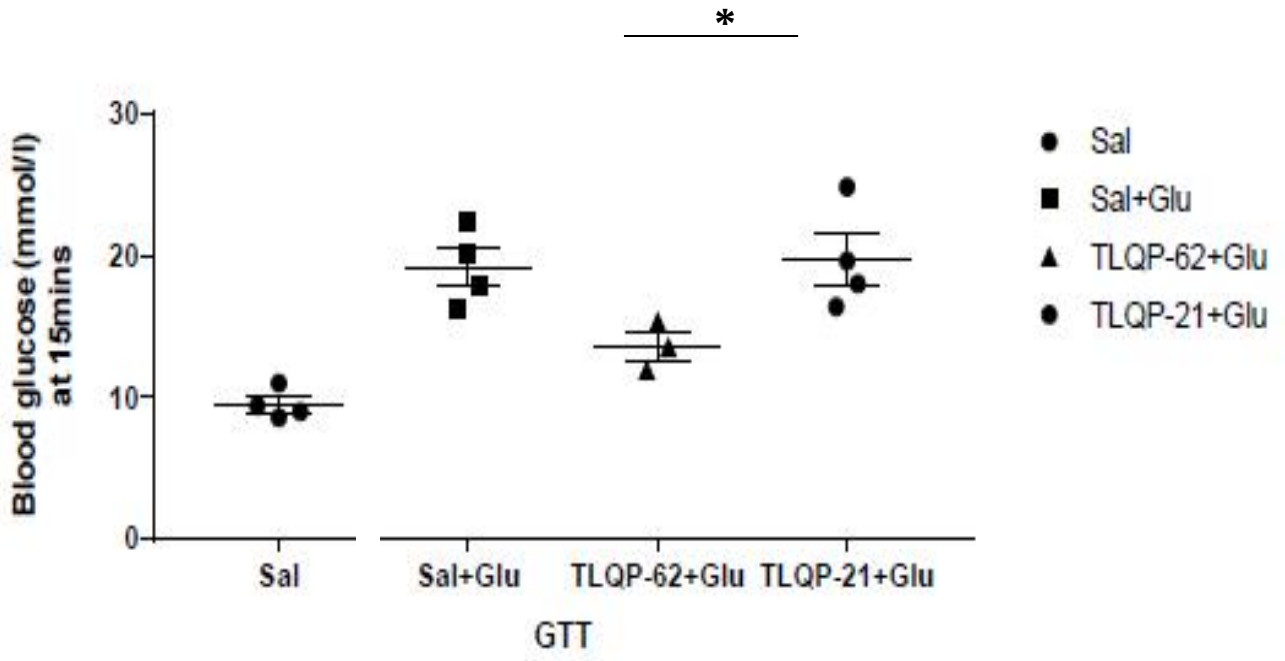

4.6.2 Effect of TLQP-62 and TLQP-21 on insulin release.

As shown in hamsters, peripheral administration of TLQP-62 induces a significant strong release of insulin into the blood, compared to controls (Sal/Glu *vs* TLQP-62/Glu $p < 0.03$; TLQP-62/Glu *vs* TLQP-21/Glu $p < 0.04$; TLQP-62/Glu *vs* only saline $p < 0.02$) and in this case, the insulin values were all measurable.

Instead, we also revealed that peripheral administration of TLQP-21 had NOT Significant effect on insuline release, the values of which are comparable to the animals that received saline (Sal/Glu *vs* TLQP-21/Glu $p > 0.05$).

Summary table of the results

SD Siberian h.

	TLQP-21 Chronic treatment	**TLQP-62** Chronic treatment	**TLQP-21** Acute treatment	**TLQP-62** Acute treatment
Food intake	Decrease	Not change	Not observed	Not observed
Meal duration	Decrease	Not change	Not observed	Not observed
Energy expenditure	Increase	Not change	Not observed	Not observed
Body weight	Decrease	Not change	Not observed	Not observed
C3aR expression	Not change	Not observed	Not observed	Not observed
Glycemia	Not observed	Decrease	Not observed	Not observed
Insulin release	Not observed	Not observed	Not observed	Not observed

LD Siberian h.

	TLQP-21 Chronic treatment	**TLQP-62** Chronic treatment	**TLQP-21** Acute treatment	**TLQP-62** Acute treatment
Food intake	Not change	Not change	Not observed	Not observed
Meal duration	Not change	Not change	Not observed	Not observed
Energy expenditure	Not change	Not change	Not observed	Not observed
Body weight	Not change	Not change	Not observed	Not observed
C3aR expression	Not change	Not observed	Not observed	Not observed
Glycemia	Not observed	Decrease	Not change	Decrease
Insulin release	Not observed	Not observed	Not observed	Increase

Mice

	TLQP-21 Acute treatment	**TLQP-62** Acute treatment	**TLQP-21** Chronic treatment	**TLQP-62** Chronic treatment
Glycemia	Not change	Decrease	Not observed	Not observed
Insulin release	Not change	Increase	Not observed	Not observed

5. GENERAL DISCUSSION

Despite the two VGF peptides TLQP-21 and TLQP-62 share the same sequence starting from the N-terminal position of the VGF precursor protein (TLQP-62 is therefore a 62 amino acid peptide that includes TLQP-21), they show different biological activities. Indeed, while TLQP-21 acts on energy balance mechanisms, TLQP-62 is able to strikingly reduce blood glucose level but not *viceversa*.

5.1 TLQP-21 activity on Siberian hamster metabolism

In the SD state hamster (lean state), the chronic peripheral administration of TLQP-21 induces an increase in the energy expenditure, oxygen consumption and carbon dioxide production. TLQP-21 furthermore significantly reduced the cumulative food intake, via decreases the meal duration in the dark phase, as well as the body weight. However, all these effects, clearly evident in the TLQP-21 treated animals in the SD phase do not longer appear in the LD phase (obesity state). It has been previously reported that chronic intracerebroventricular (i.c.v.) injection of TLQP-21 increased resting energy expenditure (EE) and rectal temperature in mice. These effects were paralleled by increased epinephrine and up-regulation of brown adipose tissue beta2-AR (beta2 adrenergic receptor) and white adipose tissue (WAT) PPAR-delta (peroxisome proliferator-activated receptor delta), beta3-AR, and UCP1 (uncoupling protein 1) mRNAs and were independent of locomotor activity and thyroid hormones (Bartolomucci et al., 2006).

Surprisingly, chronic peripheral TLQP-21 treatment was not associated with increased energy expenditure measured with indirect calorimetry, in both wild type (WT) and β-less receptors mice, a finding confirmed in a follow-up sub-chronic treatment (Cero et al., 2017), but chronic peripheral TLQP-21 treatment decrease body weight and fat mass in diet induced obesity mice, by a mechanism involving β-adrenergic receptor and C3aR1 receptor (Cero et al., 2017).

5.2 C3aR1 and the its expression in hypotalamus of Siberian hamster

The C3aR1-TLQP-21 receptor is a 54 kDa protein, member of the G-protein coupled receptor superfamily, whose role in the innate immune response has been well established (Cravedi et al., 2013). However, the receptor has recently been implicated in the regulation of obesity; C3aR1 null mice are obese, and expression of C3aR1 increases in adipocytes of obese models (Mamane et al., 2009). In this work, we have shown, by WB, that in the SD and LD Siberian hamsters there is no signal of C3aR1 expression in both white and brown adipose tissues or in pancreas islets according to the scarce role of TLQP-21 on glycemia.

Contrary to the reduction of the C3aR1 seen in the SD state within the entire hypothalamus, its expression is increased in tanycytes. Hypothalamic tanycytes are glial-like cells which line the basolateral wall of the third ventricle which act as stem cell niche (Bolborea and Dale 2013; Lewis and Ebling 2017). Hypothalamic tanycytes are pivotal for the process of weight loss in Siberian hamsters. Indeed some studies have revealed seasonal changes in tanycyte gene expression, for example an increase in deiodinase 3 enzyme in SD reducing the availability of tri-iodothyroinine (T3) in hypothalamus, resulting in body weight loss (Barrett et al., 2007; Murphy et al., 2012; Ebling, 2014). The local availability of T3 in the hypothalamus is likely to be determined by type 2 deiodinase (DIO2) that converts T4 to active T3 by outer ring deiodination, and type 3 deiodinase (DIO3), which catalyzes the conversion of T4 to rT3, and T3 to 3,3′-diiodothyronine (T2) by inner ring deiodination, inactivating T3. The balance of activities of these two enzymes thus determines the availability of active T3 hormone within the hypothalamus (Bianco et al., 2002). An *in vivo* study revealed that intra-hypothalamic T_3 administration via slow-release microimplants reduced VGF mRNA expression in the dmpARC of SD-exposed Siberian hamsters. This suggests that VGF expression *in vivo* may be regulated by availability of these hormones / ligands, which in turn are determined by the transport of their precursors and the enzymes responsible for synthesizing or degrading their active forms. Substantial evidence indicates that the generation of thyroid hormone and retinoic acid (RA) signals in the mediobasal hypothalamus is regulated by season and

photoperiod (discussed by Ebling 2014, 2015). Indeed it's been shown that T3 modulates VGF mRNA expression *in vitro* and *in vivo* (Lewis et al., 2016).

The complexity of the hormonal regulation of VGF expression that the current study has revealed may also explain the local upregulation of VGF expression in the dmpARC of SD. In the hamsters, this region has a much higher level of expression of thyroid hormone receptor b1 than the surrounding hypothalamus (Barrett et al., 2007), and Lewis et al., (2016) demonstrates that VGF mRNA expression in the dmpARC is specifically regulated by the thyroid hormone. Thus, the SD-inducing increase in DIO3 expression in tanycytes would be expected to reduce local T_3 availability, resulting in a loss of repression of VGF gene expression in the dmpARC. Intra-hypothalamic T_3 implants placed in hamsters in SD produced a rapid increase in body weight, a reflection of increased food intake and a decrease in energy expenditure (Murphy et al., 2012). Furthemore, Lewis et al. (2016) demonstrated that locally increasing hypothalamic T_3 blocks the SD-induced increase in *vgf* mRNA expression in Siberian hamsters. This is associated with a blockade of the SD-induced decrease in appetite and in weight loss, and also with the SD-induced inactivation of the reproductive axis. The correlation between *VGF* expression in the dmpARC and the physiological responses to SD was particularly highlighted in one individual hamster where the intrahypothalamic T_3 implants were ineffective in preventing any of the SD responses, probably because their placement was too rostral to influence hypothalamic function. The question now arises as to the specific role of T_3-regulated *VGF* expression in driving these seasonal responses. The function of the dmpARC itself is not clear; as one recent study found that SD-induced weight loss could occur in hamsters with lesions of this structure (Teubner et al., 2015). However, other lines of evidence suggest that increased *VGF* expression in the dmpARC could contribute to the SD-catabolic state, for example, at least one of the peptide products (TLQP-21) has been shown to reduce appetite when infused centrally into the hamster (Jethwa et al., 2007).

More importantly tanycytic perikarya are located in the ependymal layer and send long radial processes to the through the arcuate nucleus, many of which terminate in the median eminence

(Kameda et al., 2003). Electron microscopy has revealed substantial cellular remodelling in the tanycytes of Siberian hamsters exposed to SD (Kameda et al., 2003). It is thought that this process of neuroglial plasticity results in the induction of new fenestrations allowing regulation of transport of hormones and metabolites into the hypothalamus (Langlet et al., 2013; Lewis and Ebling 2017).

As we have seen, we demonstrate that chronic peripheral treatment with TLQP-21 further reduces food intake via alteration in meal size in SD animals versus saline treated control animals. In addition, treatment with TLQP-21 increases oxygen consumption and carbon dioxide production so that energy expenditure is significantly increased, independently of activity as measured in metabolic cages. This is associated with an increase in UCP1 mRNA in BAT resulting in a further reduction in bodyweight. In diet-induced obese (DIO) mice, chronic peripheral treatment with TLQP-21 exerted an anti-obesity effect, an effect which required functional β-adrenergic receptor (AR) and C3aR1 expression. Interestingly, in the Siberian hamster, SD exposure increases the sympathetic nervous system drive to adipose tissue (Bowers et al., 2005; Demas et al., 2002; Youngstrom and Bartness 1995), induces norepinephrine-induced cyclic-adenomonophosphate (cAMP) accumulation in adipocytes isolated form SD animals (Bowers et al., 2005; Youngstrom and Bartness 1995). Adipocytes from SD animals are also more sensitive to the β3-AR agonist BRL37344 and its ability to stimulate lipolysis (Bowers et al., 2005). Thus it could be proposed that the enhanced sympathetic activity to adipose tissue possibly drives the metabolic phenotype (via increased UCP1 mRNA) in SD animals treated with TLQP-21. The effects of peripheral treatment with TLQP-21 are lost in the LD maintained obese Siberian hamsters, were expression of C3ar1 is significantly reduced in tanycytes.

Hence, it could be suggested that with the inactivation of T3 due to the increase of DIO3 in tanycytes, the SD status is also maintained by production of *VGF* in the dmpARC, and the increase in C3aR1 expression in tanycytes may result in increased sensitivity of TLQP-21.

However in a work of 2018, Guo Z. et al., showed that, following i.v.-injected of TLQP-21 in rats, the uptake by the brain was negligible, suggesting that peripheral administration of this peptide does

not cross the blood-brain-barrier. This data is in line with our results obtained in the hypothalamus of the animals treated in chronic with TLQP-21 in wich there is not increase in C3aR receptor, compared to controls. Hence, we supposed that the results we obtained are due to a peripheral action of TLQP-21.

TLQP-21 is present in secretory vesicles in sympathetic nerve terminals where it co-localizes with tyrosine hydroxylase (TH), the rate limiting enzyme responsible for the biosynthesis of NE (Possenti et al., 2012). Overall, available data support a model in which TLQP-21 and NE are co-secreted and the peptide activates a C3aR1/Calcium/ERK-mediated up-regulation of NE-induced HSL activation and lipolysis (Fig. 28).

Fig. 28) Proposed model of TLQP-21 peripheral action induced pro-lipolytic effect

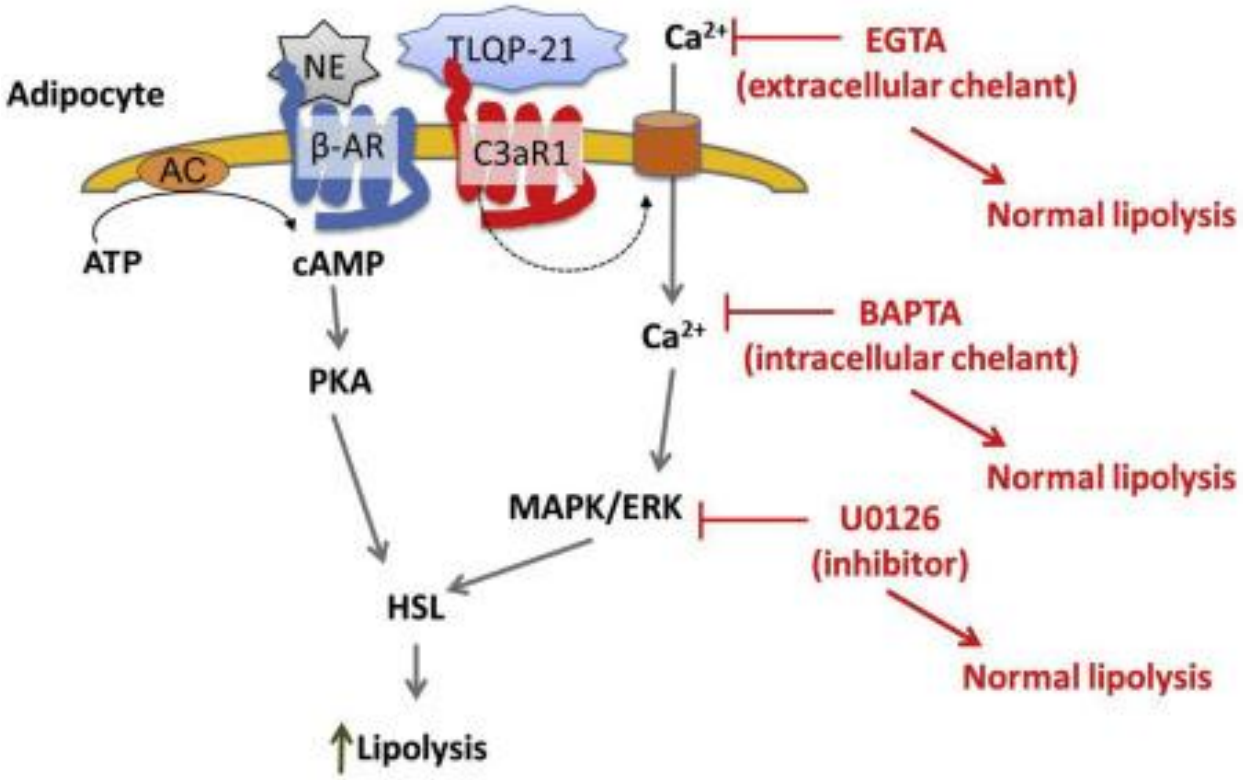

C3a derived from the circulation or adipocyte secretion and cleavage of C3 can also exert a similar effect although this remains to be characterized in light of the ASP-mediated increase in triglyceride synthesis (Murray et al., 1999). Interestingly, the TLQP-21 effect on lipolysis is opposite to NPY-

induced inhibition of adrenergic receptor-induced lipolysis (Bradley et al., 2005). Similar to TLQP-21, NPY also localizes at the sympathetic nerve terminals with TH (Giordano et al., 2005). These results suggest a peripheral regulation of sympathetically-secreted neurotransmitters and neuropeptides (NPY, Leptin, Ghrelin, TLQP-21) modulating lipolysis and appetite feedback control at hypothalamic level. It has been demonstrated that in mice chronic intracerebroventricular injection of TLQP-21 also selectively blunted the obesity-associated increase in leptin and decrease in ghrelin, a hormone produced by P / D1 cells lying on the bottom of the stomach (Bartolomucci et al., 2009). This could explain the way in which the peripheral administration of TLQP-21 lead to influence the reduction of food intake in SD hamsters, being leptin an anorectic hormone and ghrelin an orexizing hormone. Studies revealed that LD-housed hamsters were refractory to leptin treatment, whereas SD animals exhibited further substantial weight and abdominal fat loss. This species thus appears to be resistant to leptin in LD photoperiods, consistent with the observation that it gains weight and increases appetite at this phase of seasonal cycle (Rousseau et al., 2002), this could partly explain why in LD animals chronic treatment with TLQP-21 did not give any of the results we saw in the SD.

5.3 TLQP-62 on glucose related mechanism

We reported a significantly hypoglycaemic effect in animals treated with TLQP-62 either in the chronic and acute administration, not revealed instead with TLQP-21 treatment. Furthermore, in parallel to the decrease of glycemia, TLQP-62 increases insulin levels in blood.

Interestingly, in naïve or untreated SD Siberian hamsters the blood glucose levels were very high at 30 minutes from the glucose administration, contrary to the LD animals in wich they decreased after 15 minutes.

Hence it could be hypothesized that the metabolism in LD phase, or rather their ability to recover glucose from the blood is much higher than when they are in SD phase.

5.4 TLQP-62 and its possible role in intracellular mechanisms involved in insulin secretion mechanism

It has been well established that insulin is secreted in response to high glucose, but many other secretogogues can modulate its secretion through the activation of different intracellular signal pathways (Jones & Persaud, 1998). The main role of insulin in mammalian body is to induce the glucose transport into the cell. The glucose uptake by numerous cells like adipocytes or skeletal muscle cells requires activation of specific proteins called glucose transporters (Pilch, 2008). Glucose transporter type 4 (GLUT4) is responsible for about 75% of all human body glucose uptake mediated by glucose transporters (Pilch, 2008). At fasting stage, GLUT4 is localized mainly in cytoplasm. The activation of GLUT4 by PI-3 K pathway (phosphoinositide-3-kinase pathway) causes vesicle containing GLUT4 (GSV – Glut4 storage vesicle) translocation to the cell membrane and subsequently glucose uptake. The translocation of GSV is facilitated by cortical actin (Khan et al., 2002) and by numerous proteins located in GSV or in cell membrane (Saltiel et al., 2001).

Akt is a protein of 57 kDa that play a central role in insulin-stimulated glucose uptake in both muscle and adipose tissue when it is phosphorylated (pAkt). The effect of insulin on glucose uptake in peripheral tissue via Akt/pAkt is through its ability to translocate GLUTs to the cell membrane, thereby facilitating glucose uptake. Binding of insulin to its cell surface protein receptors causes subsequent tyrosine phosphorylation, resulting in phosphorylation of insulin receptor substrates on specific tyrosine residues and activation and recruitment of PI3 kinase and its downstream target Akt/pAkt (Mora et al., 2004). The Akt substrate of 160 kDa (AS160), also known as TBC1D4, is an established candidate in Akt/pAkt-induced GLUT-4 translocation in skeletal muscle. AS160 functionally maintains Rab-GTPase(s) in an active form via guanosine-50-diphosphate-loading, thereby retaining GLUT-4 within GLUT storage vesicles (Sakamoto et al., 2008). Upon activation, Akt/pAkt phosphorylates AS160, leading to a reduction in Rab-GAP (GTPase-activating protein) GTPase-activating protein) activity, promoting GLUT-4 translocation and glucose uptake (Fig. 29).

Fig. 29)

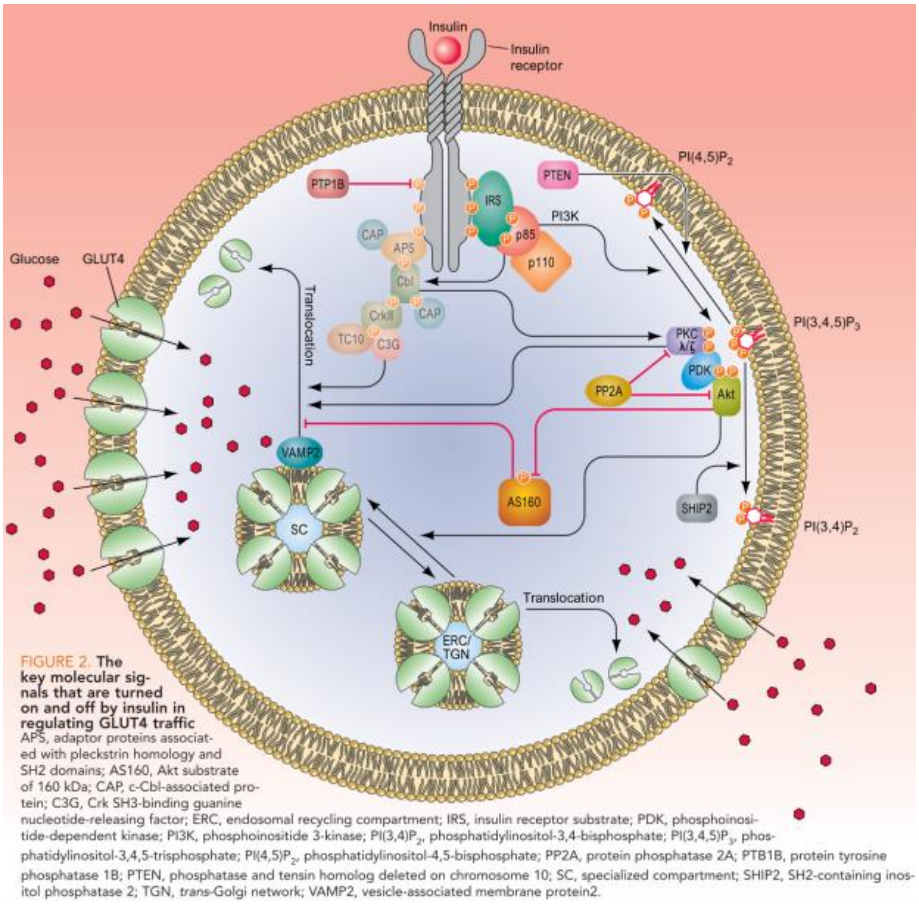

Petrocchi-Passeri in 2015, have revealed that TLQP-62 induced a significant early decrease (2-5 min) in AMPK phosphorylation, followed by its increase (10-15 min) and a further down regulation (30-60 min after). In the same work it was shown how the TLQP-62 is able to increases intracellular calcium mobilization in INS1E cells (Fig. 30).

Fig. 30) Proposed model by Petrocchi-Passeri (2015) of TLQP-62's mechanism of action. TLQP-62 ligates a not yet identified receptor (1), activating signal transduction cascades by first opening calcium channels on the membrane (2) and stimulating endoplasmic reticulum release (3), and then secondarily modulating the AMPK , PKC, and ERK pathways (4). The resulting increase in intracellular calcium concentration is permissive for the secretion of insulin (5). TLQP-62 is released along with insulin and exerts a paracrine effect (6). TLQP-62 also has an effect on gene transcription (7)

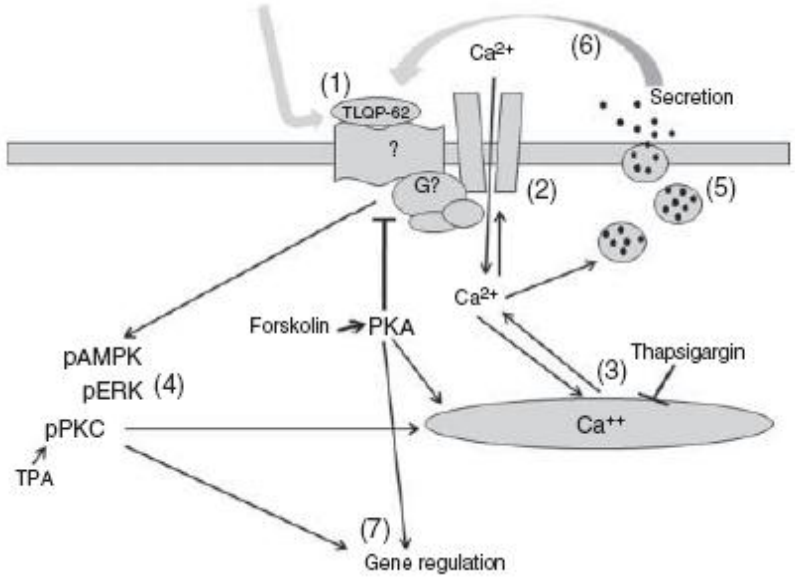

Since muscle contractions lead to activation of AMPK, it is likely that contractions/exercise lead to both increased exocytosis and decreased endocytosis of GLUT4. It appears that there may be two intracellular pools of GLUT4 and that one is recruited primarily by insulin and the other by contractions. The contraction pool is differentiated from the insulin responsive pool by consisting of mainly transferrin receptor positive structures (Coderrel et al., 1995; Lemieux et al., 2000).

The actual docking and fusion of the GLUT4 vesicles to the surface membrane is only fragmentarily understood but seems to require complex interactions between several proteins.

Much of the knowledge about mechanisms regulating docking and fusion of GLUT4 vesicles to the surface membrane comes from studies of insulin-induced GLUT4 translocation in cell culture and adipocytes, and it is tacitly assumed that the basic mechanisms during contraction-induced GLUT4 translocation in mature muscle are the same, although this is likely an over simplification.

Studies were performed in frog sartorius muscle incubated with caffeine. Caffeine causes release of calcium from the sarcoplasmic reticulum, and it also causes an increase in glucose transport. These early studies showed that the increase in muscle glucose uptake during contractions does not require membrane depolarization but only release of calcium (Holloszy et al., 1965 and 1967).

Later studies in incubated rat muscle showed increased glucose uptake when incubated with concentrations of caffeine (2.5–3.0 mM) that were too low to cause muscle contractions and alterations in adenine nucleotide status. Also, incubations with the Ca^{2+}-releasing compound *N*-(6-aminohexyl)-5-chloro-1-naphtalenesulfonamide at concentrations that did not cause muscle contraction increased transport of the non metabolizable glucose analog 3-*O*-methylglucose (3-*O*MG) 6–8 times (Wright et al., 2004 and 2005; Yang et al., 2005).

These findings suggested that calcium per se is sufficient to stimulate substantial increases in muscle glucose uptake. However, it was subsequently demonstrated by several groups that incubation with caffeine increases AMPK activation and nucleotide turnover in muscles from mice and rats even though no muscle contraction was apparent (Egawa et al., 2011; Jensen et al., 2007; Raney et al., 2008). Still, in non muscle tissues, calcium/calmodulin-dependent protein kinase kinases (CaMKKs), particularly CaMKK*β*, have been found to be able to phosphorylate AMPK on the activating Thr-172 site (Hawley et al., 2005; Hurley et al., 2005), and it could therefore be hypothesized that calcium via activation of CaMKK in muscle might be able to increase glucose uptake due to direct AMPK activation independently of energy turnover (Fig. 31).

Fig. 31) Schematic of molecular signaling involved in contraction-induced GLUT4 translocation to the surface membrane. Dotted lines indicate probable but not proven pathways

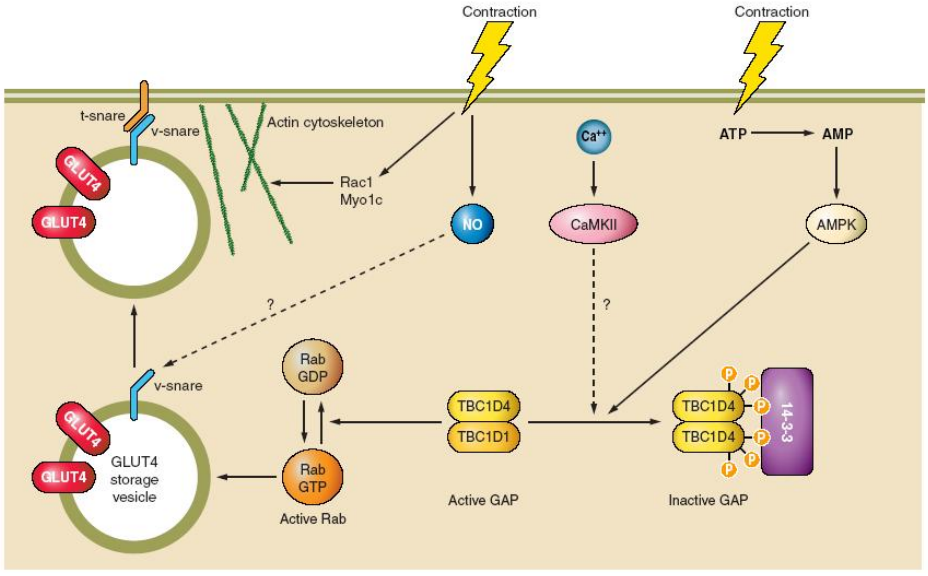

Hence, it can be speculate that TLQP-62 acts on peripheral organs such as muscle, incresing Ca^{2+} through PKA modulation to increase insulin secretion (through a paracrine action). Furthermore in peripheral tissues (as muscle) it could act increasing Ca^{2+} through PKA / Ca^{2+} related mechanisms to enhance permeability to the insulin. According to this hypothesis, an unpublished study (Corda et al., 2018) reports that in mice, TLQP-p are produced in the insulin pancreatic cells, suggesting an involvement of TLQP-p in modulating insulin secretion by autocrine /paracrine action. Furthermore they are major released in the blood in response to hyperglycaemia also suggesting an endocrine activity according to the results presented here.

6. CONCLUSIONS

The VGF derived TLQP peptides show an involvement in both physiological peripheral response to glucose (pancreas and plasma), and energy expenditure. These activities are according to the marked TLQP changes in the presence of obesity and / or diabetes both in the experimental model, and patients (D'Amato et al., 2015).

TLQP-21 and TLQP-62 act differently. As we have seen, in fact, the role of the first peptide is linked to energy expenditure, but does not acts in insulin release and blood glucose control, while TLQP-62 acts precisely in lowering blood glucose levels, but has no effect on the regulation of energy expenditure. These opposite roles are extremely fascinating and confirms that there is a fine intervention of VGF gene in these metabolic processes. Regarding TLQP-21, to define the molecular events following its receptor attack will be mandatory for future terapheutic approachs in obesity.

As for TLQP-62, demonstrating the TLQP-62 action mechanisms, that increase the entry of calcium and resulting in the glucose uptake, is a future goal. Indeed future aims will include new therapeutic strategies in patients affected by Type 1 and Type 2 diabetes and obesity, increasing receptor sensitivity to exogenous insulin, even though the mechanisms of action and the TLQP-62 receptors still need to be better understood.

To further understand the TLQP mechanisms relevance in physio-pathology or in the evolution obesity and diabetes conditions additional experiments in collaboration with Nottingham University (England) are conducting.

7. BIBLIOGRAPHY

Alder J., Thakker-Varia S., Bangasser D.A., Kuroiwa M., Plummer M.R., Shors T.J., Black I.B. 2003

Brain-derived Neurotrophic Factor-induced gene expression reveals novel actions of VGF in Hippocampal Synaptic Plasticity. The Journal of Neuroscience 23 (34): 10800-10808.

Barrett P., Ross AW., Balik A., Littlewood PA., Mercer JG., Moar KM., Sallmen T., Kaslin J., Panula P., Schuhler S., Ebling FJ., Ubeaud C., Morgan PJ. 2005

Photoperiodic regulation of histamine H3 receptor and VGF messenger ribonucleic acid in the arcuate nucleus of the Siberian hamster. Endocrinology 146(4): 1930-9.

Barrett P., Ebling FJ., Schuhler S., Wilson D., Ross AW., Warner A., Jethwa P., Boelen A., Visser TJ., Ozanne DM., Archer ZA., Mercer JG., Morgan PJ. 2007

Hypothalamic thyroid hormone catabolism acts as a gatekeeper for the seasonal control of body weight and reproduction. Endocrinology. 148(8): 3608-17.

Bartness TJ., Elliott JA., Goldman BD. 1989

Control of torpor and body weight patterns by a seasonal timer in Siberian hamsters. Am J Physiol. 257(1 Pt 2): R142-9.

Bartolomucci A., La Corte G., Possenti R., Locatelli V., Rigamonti A.E., Torsello A., Bresciani E., Bulgarelli I., Rizzi R., Pavone F., D'amato F., Severini C., Mignogna G., Giorgi A., Schininà M.E., Elia G., Brancia C., Ferri G.L., Conti R., Ciani B., Pascucci T., Dell'Olmo G., Muller E.E., Levi A., Moles A., 2006

TLQP-21, a VGF-driver peptide, increases energy expenditureand prevents the early phase of diet-induced obesity. PNAS Vol. 103 N° 39: 14584-14589.

Bartolomucci A., Possenti R., Levi A., Pavone F., Moles A. 2007

The role of the vgf gene and VGF-derived peptides in nutrition and metabolism. Genes Nutr. 2:169-80.

Bartolomucci A., Bresciani E., Bulgarelli I., Rigamonti A.E., Pascucci T., Levi A., Possenti R., Torsello A., Locatelli V., Muller E.E., Moles A. 2009

Chronic intracerebroventricular injection of TLQP-21 prevents high fat diet induced weight gain in fast weight-gaining mice. Genes.Nutr. 4:49-57.

Baybis M., Salton S.R. 1992

Nerve Growth Factor rapidly regulates VGF gene transcription through cycloheximide sensitive and insensitive pathways. FEBS lett. 308(2): 202-206.

Bianco A.C., Salvatore D., Gereben B., Berry M.J., Larsen P.R. 2002

Biochemistry, cellular and molecular biology, and physiological roles of the iodothyronine selenodeiodinases. Endocr. Rev. 23: 38–89.

Bolborea M., Dale N. 2013

Hypothalamic tanycytes: potential roles in the control of feeding and energy balance. Trends Neurosci. 36: 91-100.

Bowers RR., Gettys TW., Prpic V., Harris RB., Bartness TJ. 2005

Short photoperiod exposure increases adipocyte sensitivity to noradrenergic stimulation in Siberian hamsters. Am J Physiol Regul Integr Comp Physiol 288: R1354-1360.

Bozdagi O., Rich E., Tronel S., Sadahiro M., Patterson K., Shapiro M.L., Alberini C.M., Huntley G.W., Salton S.R.J. 2008

The neurotrophin-inducible gene Vgf regulates hippocampal function and behavior through a brain-derived neurotrophic factor-dependent mechanism. J Neurosci. 28(39): 9857-69.

Bradley R.L., Mansfield J.P., Maratos-Flier E. 2005

Neuropeptides, including neuropeptide Y and melanocortins, mediate lipolysis in murine adipocytes. Obesity Research 13(4): 653–661.

Brancia C., Cocco C., D'Amato F., Noli B., Sanna F., Possenti R., Argiolas A., Ferri G.L. 2010

Selective expression of TLQP-21 and other VGF peptides in gastric neuroendocrine cells and modulation by feeding. Journal of Endocrinology 207: 329-341.

Brancia C., Noli B., Boido M., Pilleri R., Boi A., Puddu R., Marrosu F., Vercelli A., Bongioanni P., Ferri GL., Cocco C. 2018

TLQP Peptides in amyotrophic lateral sclerosis: possible blood biomarkers with a neuroprotective role. Neuroscience 380: 152-163.

Canu N., Possenti R., Ricco A.S., Rocchi M., Levi A. 1997

Cloning, structural organization analysis, and chromosomal assignment of the human gene for the neurosecretory protein VGF. Genomics 45: 443-446.

Carrette O., Demalte I., Scherl A., Yalkinoglu O., Corthals G., Burkhard P., Hochstrasser D.F., Sanchez J.C. 2003

A panel proteomics of cerebrospinal fluid potential biomarkers for the diagnosis of Alzheimer's disease. Proteomics 3: 1486-1494.

Cero C., Razzoli M., Han R., Sahu BS., Patricelli J., Guo Z., Zaidman NA., Miles JM., O'Grady SM., Bartolomucci A. 2017

The neuropeptide TLQP-21 opposes obesity via C3aR1-mediated enhancement of adrenergic-induced lipolysis. Mol Metab 6: 148-158.

Cocco C., Brancia C., Pirisi I., D'Amato F., Noli B., Possenti R., Ferri G.L. 2007

VGF-metabolic related gene: distribution of its derived peptides in mammalian pancreatic islets. Journal of Histochemistry and Cytochemistry. 55(6): 619-628.

Coderre L., Kandror KV., Vallega G., Pilch PF. 1995

Identification and characterization of an exercise-sensitive pool of glucose transporters in skeletal muscle. J Biol Chem 46: 27584–27588.

Cravedi P., Leventhal J., Lakhani P., Ward SC., Donovan MJ., Heeger PS. 2013

Immune cell-derived C3a and C5a costimulate human T cell alloimmunity. Am J Transplant. 13(10): 2530-9.

D'Amato F., Noli B., Brancia C., Cocco C., Flore G., Collu M., Nicolussi P., Ferri G.L. 2008 Differential distribution of VGF-derived peptides in the adrenal medulla and evidence for their selective modulation. Journal of Endocrinology. 197: 359-369.

D'Amato F., Cocco C., Noli B., Cabras T., Messana I., Ferri G.L. 2012

VGF peptides upon osmotic stimuli: changes in neuroendocrine regulatory peptides 1 and 2 in the hypothalamic-pituitary-axis and plasma. Journal of Chemical Neuroanatomy 44: 57-65.

D'Amato F., Noli B., Angioni L., Cossu E., Incani M., Messana I., Manconi B., Solinas P., Isola R., Mariotti S., Ferri G.L., Cocco C. 2015

VGF peptide profiles in type 2 Diabetic patiens' plasma and in obese mice. PLoS ONE 10 (11).

Demas GE., Bowers RR., Bartness TJ., Gettys TW. 2002

Photoperiodic regulation of gene expression in brown and white adipose tissue of Siberian hamsters (Phodopus sungorus). Am J Physiol Regul Integr Comp Physiol. 282: R114-121.

Ducruet AF., Zacharia BE., Sosunov SA., Gigante PR., Yeh ML., Gorski JW., Otten ML., Hwang RY., DeRosa PA., Hickman ZL. 2012

Complement inhibition promotes endogenous neurogenesis and sustained anti-inflammatory neuroprotection following reperfused stroke. PLoS One 7 e38664.

Ebling FJP. 1994

Photoperiodic differences during development in the Dwarf Hamsters Phodopus-Sungorus and Phodopus-Campbelli. General and Comparative Endocrinology 95: 475-482.

Ebling FJ. 2014

On the value of seasonal mammals for identifying mechanisms underlying the control of food intake and body weight. Horm Behav. 66(1): 56-65.

Ebling FJ. 2015

Hypothalamic control of seasonal changes in food intake and body weight. Front Neuroendocrinol. 37: 97-107.

Egawa T., Hamada T., Ma X., Karaike K., Kameda N., Masuda S., Iwanaka N., Hayashi T. 2011

Caffeine activates preferentially alpha1-isoform of 5'AMP-activated protein kinase in rat skeletal muscle. Acta Physiol. 201: 227–238.

Fargali S., Scherer T., Shin AC., Sadahiro M., Buettner C., Salton SR. 2012

Germline ablation of VGF increases lipolysis in white adipose tissue. J Endocrinol. 215(2): 313-22.

Ferri G.L., Noli B., Brancia C., D'Amato F., Cocco C. 2011

VGF: An inducible gene product, precursor of a diverse array of neuroe-edocrine peptides and tissue-specific disease biomarkers. J.of Chem. Neuroanatomy 42: 249-261.

Francis K., Lewis BM., Akatsu H., Monk PN., Cain SA., Scanlon MF., Morgan BP., Ham J., Gasque P. 2003

Complement C3a receptors in the pituitary gland: a novel pathway by which an innate immune molecule releases hormones involved in the control of inflammation. FASEB J. 17(15): 2266-8.

Fujihara H., Sasaki K., Mishiro-Sato E., Ohbuchi T., Dayanithi G., Yamasaki M., Minamino N. 2012

Molecular characterization and biological function of neuroendocrine regulatory peptide-3 in the rat. Endocrinology 153 (3): 1377-1386.

Giordano A., Frontini A., Murano I., Tonello C., Marino M.A., Carruba M.O. 2005
Regional-dependent increase of sympathetic innervation in rat white adipose tissue during prolonged fasting. Journal of Histochemistry & Cytochemistry 53(6): 679–687.

Guo Z., Sahu B., He R., Finan B., Cero C., Verardi R., Razzoli M., Veglia G., Di Marchi R., Miles J., Bartolomucci A. 2018
Clearance kinetics of the VGF-derived neuropeptide TLQP-21. Neuropeptides : In Press.

Hahm S., Mizuno T.M., Wu T.I., Wisor J.P., Priest C.A., Kozoc C.A., Boozer C.N., Peng B., Mcevoy R.C., Good P., Kelley K.A., Takahashi J.S., Pintar J.E., Roberts J.L., Mobbs C.V., Salton S.R.J. 1999
Targeted deletion of the gene indicates that the encoded secretory peptide precursor plays a novel role in the regulation of energy balance. Neuron. (3): 537-48.

Hahm S., Fekete C., Mizuno T.M., Windsor J., Yan H., Boozer C.N., Lee C., Elmquist J.K., Lechan R.M., Mobbs C.V., Salton S.R.J. 2002
VGF is required for obesity induced by diet, gold thioglucose treatment, and agouti ans is differentially regulated in Pro-opiomelanocortin- and Neuropeptide Y- containing Arcuate Neurons in response to fasting. J. Neurosci. 22(16): 6929-6938.

Hannedouche S., Beck V., Leighton-Davies J., Beibel M, Roma G., Oakeley EJ., Lannoy V., Bernard J., Hamon J., Barbieri S., Preuss I., Lasbennes MC., Sailer AW., Suply T., Seuwen K., Parker CN., Bassilana F. 2013

Identification of the C3a receptor (C3AR1) as the target of the VGF-derived peptide TLQP-21 in rodent cells. Biol Chem. 288 (38): 27434-43.

Hawley R.J., Scheibe R.J., Wagner J.A. 1992

NGF induces the expression of the VGF gene through a c-AMP response element. J. Neurosci. 12: 2573-2781.

Hawley SA, Pan DA, Mustard KJ, Ross L, Bain J, Edelman AM, Frenguelli BG, Hardie DG. 2005

Calmodulin-dependent protein kinase kinase-beta is an alternative upstream kinase for AMP-activated protein kinase. Cell Metab. 2: 9–19.

Herschman H.R. 1989

Extracellular signals, transcriptional responses and cellular specificity. Trends Biol. Sci. 14: 455-458.

Holloszy JO., Narahara HT. 1965

Studies of tissue permeability. J Biol Chem. 240: 3493–3500.

Holloszy JO., Narahara HT. 1967

Nitrate ions: potentiation of increased permeability to sugar associated with muscle contractions. Science 155: 573–575, 1967.

Huang J.T., Leweke F.M., Oxley D., Wang L., Harris N., Koethe D., Gerth C.W., Nolden B.M., Gross S., Schreiber D., Reed B., Bahn S. 2006

Disease biomarkersin cerebrospinal fluid of patients with first-onset of psychosis. PloS Med.3 e428.

Huang J.T., Leweke F.M., Tsang T.M., Koethe D., Kranaster L., Gerth C.W., Gross S., Schreiber D., Ruhrmann S., Schultze-Lutter L., Klosterklotter J., Holmes E., Bahn S. 2007

CSF metabolic and proteomic profiles in patients prodromalfor psychosis. PloS One 2 e756.

Hunsberger J.G., Newton S.S., Bennett A.H., Duman C.H., Russell D.S. Salton S.R., Duman R.S. 2007

Antidepressant action of the exercise-regulated gene VGF. Nature Medicine Vol.13 N°12 1476-1482.

Hurley RL., Anderson KA., Franzone JM., Kemp BE., Means AR., Witters LA. 2005

The Ca^{2+} / calmodulin-dependent protein kinase kinases are AMP-activated protein kinase kinases. J. Biol. Chem. 280: 29060–29066.

Jensen TE., Rose AJ., Hellsten Y., Wojtaszewski JF., Richter EA. 2007

Caffeine-induced Ca^{2+} release increases AMPK-dependent glucose uptake in rodent soleus muscle. Am J Physiol Endocrinol. Metab. 293: E286–E292.

Jethwa P.H., Warner A., Nilaweera K.N., Bramenld J.M., Keyte J.W., Carter W.G., Bolton N., Bruggraber M., Morgan P.J., Barrett P., Ebling F.J.P. 2007

VGF-derived peptide, TLQP-21, regulates food intake and body weight in Siberian hamsters. Endocrinology 148(8): 4044-4055.

Jethwa P.H., Ebling F.J.P. 2008

Role of VGF-derived peptides in the control of food intake, body weight and reproduction. Neuroendocrinology. 88(2): 80-87.

Jones PM., Persaud SJ. 1998

Protein kinases, protein phosphorylation, and the regulation of insulin secretion from pancreatic beta-cells. Endocr Rev. (4): 429-61.

Kameda Y., Arai Y., Nishimaki T. 2003

Ultrastructural localization of vimentin immunoreactivity and gene expression in tanycytes and their alterations in hamsters kept under different photoperiods. Cell Tissue Res. 314: 251-262.

Khan A.H., Pessin J.E. 2002

Insulin regulation of glucose uptake: a complex interplay of intracellular signaling pathway. Diabetologia 45: 1475-1483.

Klos A., Tenner AJ., Johswich KO., Ager RR., Reis ES., Köhl J. 2009

The role of the anaphylatoxins in health and disease. Mol Immunol. 46(14): 2753-66.

Langlet F., Levin BE., Luquet S., Mazzone M., Messina A., Dunn-Meynell AA., Balland E., Lacombe A., Mazur D., Carmeliet P., et al. 2013

Tanycytic VEGF-A boosts blood-hypothalamus barrier plasticity and access of metabolic signals to the arcuate nucleus in response to fasting. Cell Metab. 17: 607-617.

Lemieux K., Han XX., Dombrowski L., Bonen A., Marette A. 2000

The transferrin receptor defines two distinct contraction-responsive GLUT4 vesicle populations in skeletal muscle. Diabetes 49: 183–189.

Lemmens R., Larsson O., Berggren PO., Islam MS. 2001

Ca^{2+}-induced Ca^{2+} release from the endoplasmic reticulum amplifies the Ca^{2+} signal mediated by activation of voltage-gated L-type Ca^{2+} channels in pancreatic β-cells. Journal of Biological Chemistry 276 9971–9977.

Levi A., Eldridge J.D., Paterson B.M. 1985

Molecular cloning of a gene sequence regulated by nerve growth factor. Science 229: 393-395.

Lewis JE, Brameld JM, Jethwa PH. 2015

Neuroendocrine Role for VGF. Front Endocrinol (Lausanne); review 6: 3.

Lewis JE., Brameld JM., Hill P., Wilson D., Barrett P., Ebling FJ., Jethwa PH. 2016

Thyroid hormone and vitamin D regulate VGF expression and promoter activity. J Mol Endocrinol. 56: 123-134.

Lewis JE., Ebling FJ. 2017

Tanycytes As Regulators of Seasonal Cycles in Neuroendocrine function. Front Neurol. 8: 79.

Lim J., Berezniuk I., Che F-Y., Parikh R., Biswas R., Pan H., Fricker L.D. 2006

Altered neuropeptide processing in prefrontal cortex of $Cpe^{fat\ /\ fat}$ mice: implications for neuro peptide discovery. Journal of Neurochemistry 96: 1169-1181.

Liu J. W., Andrews P. C., Mershon J. L., Yan C., Allen D. L., Ben-Jonatan N. 1994

Peptide V: a VGF-derived neuropeptide purified from bovine posterior pituitary. Endocrinology 135: 2742-2748.

Mamane Y., Chan C. C., Lavallee G., Morin N, Xu L. J., Huang J. Q., Gordon R., Thomas W., Lamb J., Schadt E. E., Kennedy B. P., Mancini J. A. 2009

The C3a Anaphylatoxin Receptor is a key mediator of insulin resistance and functions by modulating adipose tissue macrophage infiltration and activation. Diabetes 58(9): 2006-2017

Miyatake Y., Okumura N., Nagai K., Nakagawa H. 1993

The signal transduction pathway for VGF expression due to NGF is different from that due to b FGF in PC12 cell. Biochem Mol. Biol. Int. 30: 231-236.

Moin A.S., Yamaguchi H., Rhee M., Kim J-W., Toshinai K., Waise T.M.Z., Naznin F., Matsuo T., Sasaki K., Minamino N., Yoon K-H., Nakazato M. 2012

Neuroendocrine regulatory peptide-2 stimulates glucose-induced insulin secretion in vivo and in vitro. Biochem Biophys Res Commun. 428(4): 512-7.

Mora A., Komander D., Van Aalten DM., Alessi DR. 2004

PDK1, the master regulator of AGC kinase signal transduction. Semin Cell Dev Biol. 15(2): 161-70.

Murphy M., Jethwa PH., Warner A., Barrett P., Nilaweera KN., Brameld JM., Ebling FJ. 2012

Effects of manipulating hypothalamic triiodothyronine concentrations on seasonal body weight and torpor cycles in Siberian hamsters. Endocrinology. 153(1): 101-12.

Murray I., Köhl J., Cianflone K. 1999

Acylation-stimulating protein (ASP): structure-function determinants of cell surface binding and triacylglycerol synthetic activity. Biochemical Journal. 342(Pt 1): 41-48.

Naoya Matsumoto, Abhigyan Satyam, Mayya Geha, Peter H. Lapchak, Jurandir J. Dalle Lucca, Maria G. Tsokos, George C. Tsokos. 2017

C3a enhances the formation of intestinal organoids through C3aR1. Front Immunol. 8: 1046.

Noli B., Brancia C., Pilleri R., D'Amato F., Messana I., Manconi B., Ebling F.J., Ferri G.L., Cocco C. 2015

Photoperiod Regulates vgf-Derived Peptide Processing in Siberian Hamsters. PLoS One 10(11): e0141193.

Petrocchi-Passeri P., Cero C., Cutarelli A., Frank C., Severini C., Bartolomucci A., Possenti R. 2015

The VGF-derived peptide TLQP-62 modulates insulin secretion and glucose homeostasis. Journal of Molecular Endocrinology 54: 227-239.

Pilch R.F. 2008

The mass action hypothesis: formation of Glut4 storage vesicles, a tissue-specific, regulated exocytic compartment. Acta Physiol. 192: 89-101.

Pinilla L., Pineda R., GaytanF., Romero M., Garcia-Galiano D., Sanchez-Garrido M.A., Ruiz-PinoF., Tene-Sempere T., Aguilar E. 2011

Characterization of the reproductive effects of the anorexigenic VGF-derived peptide TLQP-21: in vivo and in vitro studies in male rats. Am. J. Physiol. EndocrinolMAteb. 300: 837-847.

Possenti R., Di Rocco G., Nasi S., Levi A. 1992

Regulatory elementsin the promoter region of vgf, a nerve growth factor–inducibile gene. Proc. Natl. Acad. Sci. 89: 3815-3819.

Possenti R., Rinaldi A.M., Ferri G-L., Borboni P., Trani E., Levi A. 1999

Expression, processing and secretion of the neuroendocrine VGF Peptides by INS-1 cells. Endocrinology Vol 140 n. 8 : 3727-3735.

Possenti R., Muccioli G., Petrocchi P., Cero C., Cabassi A., Vulchanova L., Riedl MS., Manieri M., Frontini A., Giordano A., Cinti S., Govoni P., Graiani G., Quaini F., Ghè C., Bresciani E., Bulgarelli I., Torsello A., Locatelli V., Sanghez V., Larsen BD., Petersen JS., Palanza P., Parmigiani S., Moles A., Levi A., Bartolomucci A. 2012

Characterization of a novel peripheral pro-lipolytic mechanism in mice: role of VGF-derived peptide TLQP-21. Biochem J. 441 (1): 511-22.

Raney MA., Turcotte LP. 2008

Evidence for the involvement of CaMKII and AMPK in Ca^{2+}-dependent signaling pathways regulating FA uptake and oxidation in contracting rodent muscle.

J. Appl. Physiol. 104: 1366–1373.

Rizzi R., Bartolomucci A., Moles A., D'Amato F., Sacerdote P., Levi A., La Corte G., Ciotti M.T., Possenti R., Pavone F. 2008

The VGF-derived peptide TLQP-21: a new modulatory peptide for inflammatory pain. Neuroscience Letters 441: 129-133.

Rousseau K., Atcha Z., Ramon F.A., Le Rouzic P., Stirland J.A., Ivanov T.R., Ebling F.J., Klingenspor M., S. I. Loudon A. S. 2002

Photoperiodic regulation of leptin resistance in the seasonally breeding Siberian hamster (Phodopus sungorus). Endocrinology 143 (8): 3083-3095.

Sadahiro M., Erickson C., Lin W-J., Shin A.C., Razzoli C.J., Fargali S., Gurney A., Kelley K.A., Buettner C., Bartolomucci A., Salton S.R. 2015

Role of VGF-derived Carboxy-terminal peptides in energy balance and reproduction: analysis of "humanized" Knockin Mice Expressing full-length or truncated VGF. Endocrinology 5: 1724-1738.

Saderi N., Cazarez-Marquez F., Bujis F.N., Salgado-Delgado R. C., Guzman-Ruiz M., Basualdo M.C., Escobar C., Bujis R.M. 2014

A role for VGF in the hypothalamic Arcuate and Paraventricular nuclei in the control of energy homeostasis. Neuroscience 265: 184-195.

Sakamoto K., Holman GD. 2008

Emerging role for AS160/TBC1D4 and TBC1D1 in the regulation of GLUT4 traffic. Am J Physiol Endocrinol Metab. 295(1): E29-37.

Saltiel A., Kahn C.R. 2001

Insulin signaling and the regulation of glucose and lipid metabolism. Nature 414: 799-806.

Salton S.R.J., Fischberg D.J. Dong K. 1991

Structure of the gene encoding VGF, a nervous system-specific mRNA that is rapidly and selectivelyinduced by nerve growth factor in PC12 cells. Mol. Cell. Biol. 11: 2335-2349.

Salton S.R.J., Ferri G.L., Hahm S., Snyder S.E., Wilson A.J., Possenti R., Levi A. 2000
VGF: A novel role for this neuronal and neuroendocrine polypeptide in the regulation of energy balance. Front. Neuroendocrinol. 21: 199-219.

Schisler J.C., Jensen P.B., Taylor D.G., Becker T.C., Knop F.K., TakekawaS., German M., Weir G.C., Lu D., Mirmira R.G., Newgard C.B. 2005
The Nkx6.1 homeodomain transcription factor supresses glucagon expressionand regulates glucose –stimulated insulin secretionin islet β-cells. Proc. Natl. Acad. Sci.102:7297-7302.

Schisler J.C., Fueger P.T., Babu D.A., Hohmeier H.E., Tessem J.S., Lu D., Becker T.C., Naziruddin B., Levy M., Mirmira R.G., Newgard C.B. 2008
Stimulation of human and rat islet β-cell proliferationwith retentionof functionby the homeodomain transcription factor Nkx6.1. Mol. Cell. Biol. 28: 3465-3476.

Schneider CA., Rasband WS., Eliceiri KW. 2012
NIH Image to ImageJ: 25 years of image analysis. Nat Methods 9: 671-675.

Severini C., La Corte G., Improta G., Broccardo M., Agostini S., Petrella C., Sibilia V., Pagani F., Guidobono F., Bulgarelli I.; Ferri G.L., Brancia C., Rinaldi A.M., Levi A., Possenti R. 2009
In vitro and in vivo pharmacological role of TLQP-21, a VGF-derived peptide,in the regulationof rat gastric motor functions. British Journal of pharmacology 157(6): 984-993.

Stark M., Danielsson O., Griffiths W. J., Jornvall H. and Johansson J. 2001
Peptide repertoire of human cerebrospinal fluid: novel proteolytic fragments of neuroendocrine proteins. J. Of Chromatog. 754: 357–367.

Stephens S.B., Schisler J.C., Hohmeier H.E., An J., Sun A.Y., Pitt G.S., Newgard C.B. 2012
A VGF-Derived peptide attenuates development of type 2 diabetes via Enhancement of Islets β-cell survival and function. Cell Metabolism 16: 33-43.

Succu S., Cocco C., Mascia M.S., Melis T., Melis M.R., Possenti R., Levi A., Ferri G-L., Argiolas A., 2004
Pro-VGF-derived peptides induce penile erection in male rats: possible involvement of oxytocin. Federation of European Neuroscience Societies, European Journal of Neuroscience 20: 3035–3040.

Succu S., Mascia M.S., Melis T., Sanna F., Melis M.R., Possenti R., Argiolas A. 2005
Pro-VGF-derived peptides induce penile erection in male rats: Involvement of paraventricular nitric oxide. Neuropharmacology 49: 1017-1025.

Teubner BJ., Leitner C., Thomas MA., Ryu V., Bartness TJ. 2015
An intact dorsomedial posterior arcuate nucleus is not necessary for photoperiodic responses in Siberian hamsters. Hormones and Behavior 70: 22–29.

Thakker-Varia S., Jernstedt Krol J., Nettleton J., Bilimoria P.M., Bangasser D.A., Shors T.J., Black I.B., Alder J. 2007
The neuropeptide VGF produces antidepressant-Like behavioral effect and enhances proliferation in the hippocampus. The Journal of Neuroscience 30(28): 9368-9380.

Toshinai K., Yamaguchi H., Kageyama H., Matsuo T., Koshinaka K., Sasaki K., Shioda S., Minamino N., Nakazato M. 2010

Neuroendocrine regulatory peptide-2 regulates feeding behavior via the orexin system in the hypothalamus. American Journal of Physiology Endocrinology and metabolism 299: 394-401.

Trani E., Ciotti T., Rinaldi A.M., Canu N., Ferri G.L., Levi A., Possenti R. 1995

Tissue-specific processing of the neuroendocrine protein VGF. Journal of Neurochemistry 65: 2441-2449.

Trani E., Giorgi A., Canu N., Amadoro G., Rinaldi A.M., Halban P.A., Ferri G.L., Possenti R., Schininà M.E., Levi A. 2002

Isolation and characterization of VGF peptides in rat brain. Role of PC1/3 and PC2 in the maturation of VGF precursor. Journal of Neurochemistry 81: 565-574.

Watson E., Hahm S., Mizuno TM., Windsor J., Montgomery C., Scherer PE., Mobbs CV., Salton SR. 2005

VGF ablation blocks the development of hyperinsulinemia and hyperglycemia in several mouse models of obesity. Endocrinology 12: 5151-63.

Watson E., Fargali S., Okamoto H., Sadahiro M., Gordon RE., Chakraborty T., Sleeman MW., Salton SR. 2009

Analysis of knockout mice suggests a role for VGF in the control of fat storage and energy expenditure. BMC Physiol. 9: 19.

Wright DC., Hucker KA., Holloszy JO., Han DH. 2004

Ca^{2+} and AMPK both mediate stimulation of glucose transport by muscle contractions. Diabetes 53: 330 –335.

Wright DC., Geiger PC., Holloszy JO., Han DH. 2005

Contraction- and hypoxia-stimulated glucose transport is mediated by a Ca^{2+}-dependent mechanism in slow-twitch rat soleus muscle. Am J Physiol Endocrinol Metab. 288: E1062–E1066.

Yamaguchi H., Sasaki K., Satomi Y., Shimbara T., Kageyama H., Mondal M.S., Toshinai K., Date Y., Gonzales L.J., Shioda S., Takao T., Nakazato M., Minamino N. 2007

Peptidomic identification and biological validation of neuroendocrine regulatory peptide-1 and -2. The Journal of Biological Chemistry Vol. 282 N°36: 26354-26360.

Youngstrom TG., Bartness TJ. 1995

Catecholaminergic innervation of white adipose tissue in Siberian hamsters. Am J Physiol. 268: R744-751.

Zhang X., Che F-Y., Berezniuk I., Sonmez K., Toll L., Fricker L.D. 2008

Peptidomics of $Cpe^{fat/fat}$ mouse brain region: implication for neuropeptide processing. Journal of Neurochemistry 107: 1596-1613.